ELECTRONIC SUPPLEMENTARY INFORMATION

Orthogonal Self-Assembly of a Trigonal Triptycene Triacid: Signaling of Exfoliation of Porous 2D Metal-Organic Layers by Fluorescence and Selective CO_2 Capture by the Hydrogen-Bonded MOF

Pujari Chandrasekhar, Arindam Mukhopadhyay, Govardhan Savitha and
Jarugu Narasimha Moorthy*

Department of Chemistry, Indian Institute of Technology, Kanpur-208016, INDIA

E-mail: moorthy@iitk.ac.in

CONTENTS

General Aspects. ^{1}H NMR spectra were recorded with a 400 MHz spectrometer. ^{13}C NMR spectra were recorded with a 100 MHz NMR spectrometer with complete proton decoupling. IR spectra were recorded using FT-IR spectrophotometer. Mass spectral analyses were carried out with on a ESI-^{Q}TOF Instrument. Thermogravimetric analyses were carried out under a N_2 atmosphere with a heating rate of 10 °C/min. The ultrasonication-induced exfoliation experiments were performed with the help of a ultrasonicator bath operating at a frequency of 25 kHz. All the solvents were freshly distilled prior to use. All the HPLC grade solvents used for MOF synthesis and fluorescence studies were purchased from Merck, India. The metal salts were obtained from Sigma-Aldrich, India. Low-pressure volumetric gas adsorption measurements were performed at different temperatures for N_2, CO_2 and H_2 by maintaining the temperatures using a cryo-cooler with pressures ranging from 0 to 1 bar on a Quantachrome Autosorb iQ automated gas sorption analyzer. The high pressure gas adsorption studies were performed with a Quantachrome iSorb HP1 analyzer. XPS analysis was done by using the PHI 5000 Versa Prob II, FEI Inc. with C60 sputter Guns.

Synthesis of the Triacid Linker H_3TPA

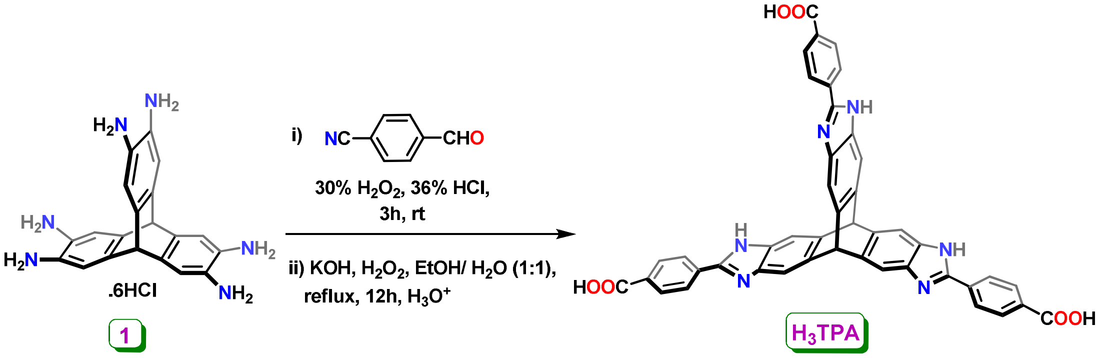

p-Carboxyphenylimidazole-Annulated Triptycene, H_3TPA.

A 100 mL round-bottomed flask was charged with 2,3,6,7,14,15-hexaammoniumtriptycene hexachloride **1** (1.25 g, 1.81 mmol), 4-formylbenzonitrile (1.42 g, 10.86 mmol) and 25 mL of acetonitrile. To this mixture were added 8% HCl (10 mL) and 30% H_2O_2 (8 mL) slowly at rt over a period of 5 min. The whole reaction mixture was allowed to stir at rt for 3 h. After this period, the resultant brown colored precipitate was filtered and washed with acetonitrile. It was further triturated with 50% EtOAc/pet.ether to remove any organic impurities. The solid material was filtered and dried to obtain a brown colored solid.

IR, ^{1}H and ^{13}C Spectroscopic analyses of the product at this stage was revealed it to be a complex mixture of triptycene-trinitrile and triptycene-amides derived by partial hydrolysis. Consequently, unambiguous characterization at this stage was deemed futile. Therefore, the product mixture as such was subjected to exhaustive hydrolysis as follows.

To a solution of the brown colored solid (1.20 g, 1.72 mmol) in 50 mL of ethanol/H_2O (1:1, v/v) mixture was added KOH (0.79 g, 14.18 mmol) and 2 mL of 30% H_2O_2 aqueous solution. The contents were stirred at 90 ^{o}C for 24 h. Subsequently, ethanol was evaporated under reduced pressure and the resultant solution was diluted with 20 mL of distilled water. This solution was then washed twice with EtOAc to remove organic impurities and the aqueous phase was acidified with 17% aq. HCl up to a *p*H of 2-3.The brown-colored precipitate thus formed was filtered, triturated with 50% EtOAc/pet. ether and filtered once again to obtain **H_3TPA** as a brown solid, yield 94%.

In a number of synthesis experiments, we observed that the product isolated by acidification only up to a *p*H of ca. 5 was found to be completely insoluble. In contrast, that isolated by acidification up to a *p*H of 2-3 was found to be better soluble in solvents such as DMSO. Clearly, the product at this *p*H is partially protonated. The ^{1}H NMR, ^{13}C NMR and ESI-MS spectral analyses revealed the product to be a mono-protonated triacid, i.e., **H_3TPA-H^+**. When the ^{1}H and ^{13}C NMR spectra of the triacid were recorded in DMSO by adding a drop of TFA, highly simplified spectra corresponding to the compound with tri-protonation of the benzimidazole moieties of triptycene-triacid, i.e., **H_3TPA-3H^+** was observed. Indeed, acidification of **H_3TPA-H^+** with TFA led to the formation of **H_3TPA-3H^+ 3CF_3COO^-** salt, which was further characterized by recording the melting point, IR and ESI-MS analyses.

To further establish the structure of **H_3TPA-3H^+** salt unambiguously, single crystal X-ray structure determination was carried out. The single crystals of suitable quality were successfully grown for the latter in TFA. In Figure S1 is shown a perspective diagram of the molecular structure of the salt, which shows that all the imidazole groups are protonated. It should be noted that the salt crystallizes with one additional molecule of TFA included as a guest in the lattice.

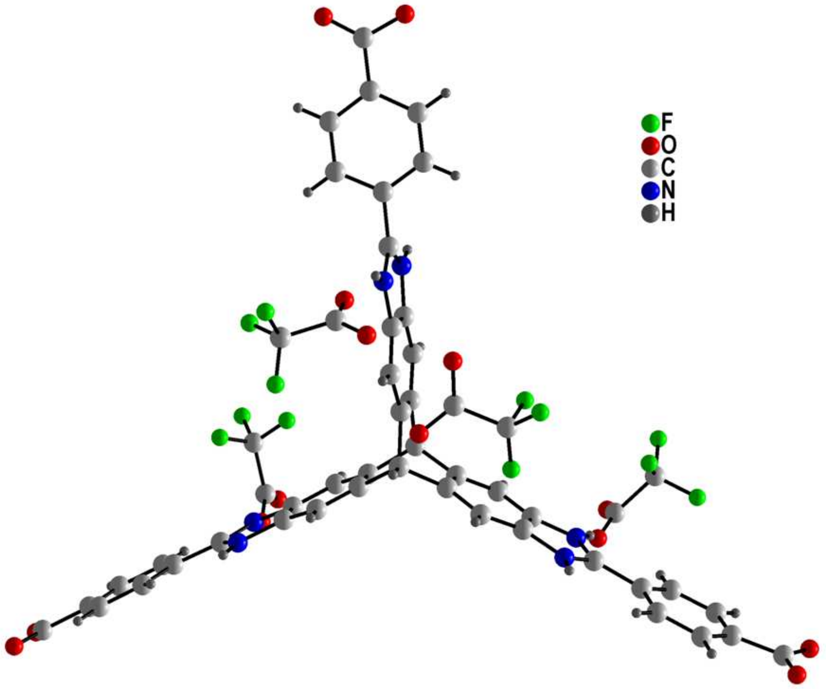

Figure S1. Single crystal X-ray structure of [**H_3TPA-3H^+ 3CF_3COO^-]•CF_3COOH**. Notice that the one TFA molecule is additionally present as a guest besides three TFA anions.

H_3TPA-3H^+: mp > 300 °C; IR (KBr) cm^{-1} 3454, 1636, 1384, 1189, 1093; ^1H NMR (400 MHz, DMSO-d_6) δ 6.36 (s, 2H), 8.04 (s, 6H), 8.13– 8.23 (AA'BB', 12H); ^{13}C NMR (100 MHz, DMSO-d_6) δ 52.8, 110.9, 127.6, 128.7, 130.9, 131.1, 135.2, 143.4, 148.9, 167.2; ESI-MS *m/z* $[M+3H]^{3+}$ calcd for $C_{44}H_{29}N_6O_6$ 245.7382, found 245.7342.

H_3TPA-H^+: mp > 300 °C; IR (KBr) cm^{-1} 3390, 3039, 2831, 1697, 1611, 1383, 1260; ^1H NMR (400 MHz, DMSO-d_6) δ 6.39 (s, 2H), 8.02 (m, 6H), 8.17 (d, J = 8.4 Hz, 6H), 8.41 (d, J = 8.4 Hz, 6H); ^{13}C NMR (100 MHz, DMSO-d_6) δ 52.1, 110.2, 128.0, 128.2, 129.6, 130.4, 131.2, 134.0, 134.6, 142.5, 148.0, 166.6, 166.8; ESI-MS *m/z* $[M+H]^+$ calcd for $C_{44}H_{27}N_6O_6$ 735.1992, found 735.1997.

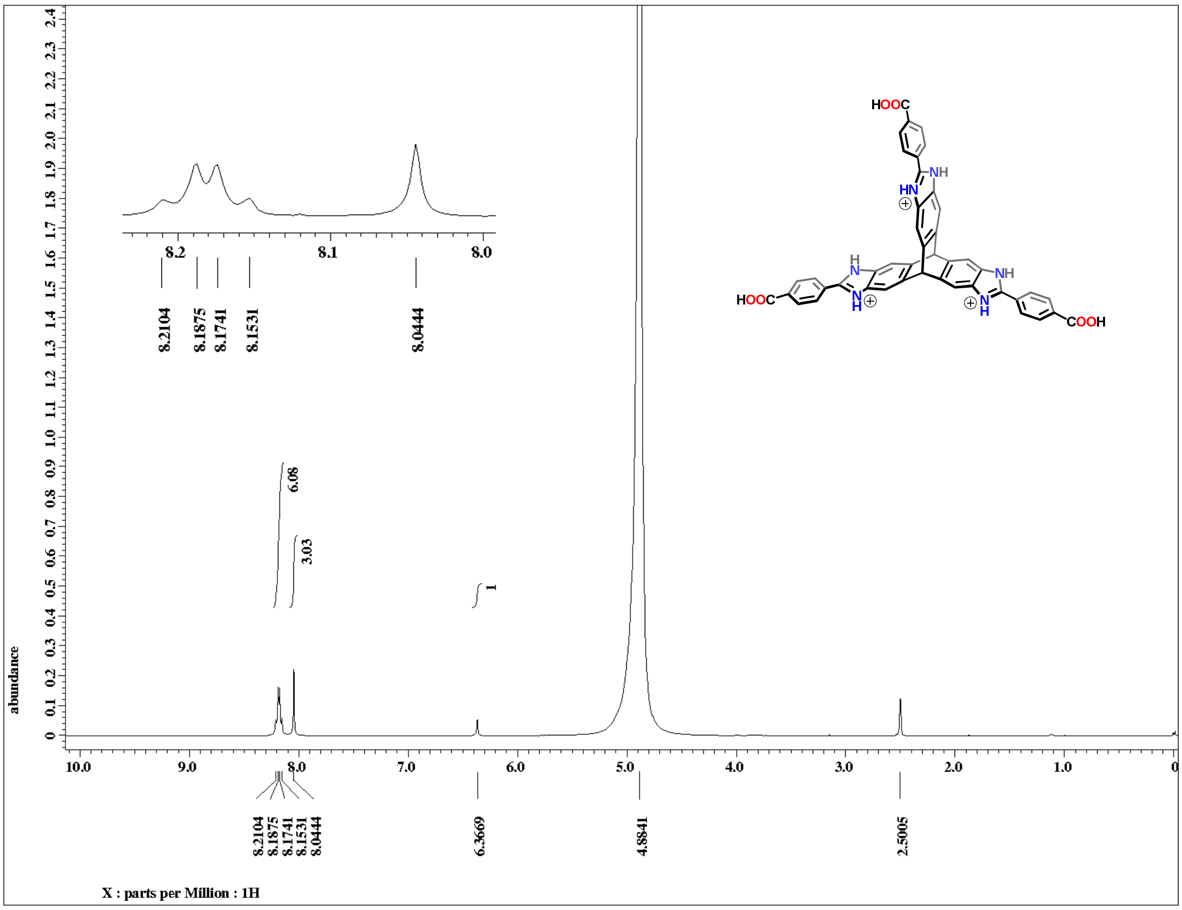

Figure S2. ^{1}H NMR (400 MHz, DMSO-d_6 + $\mathbf{CF_3COOH}$) spectrum of $\mathbf{H_3TPA\text{-}3H^+}$.

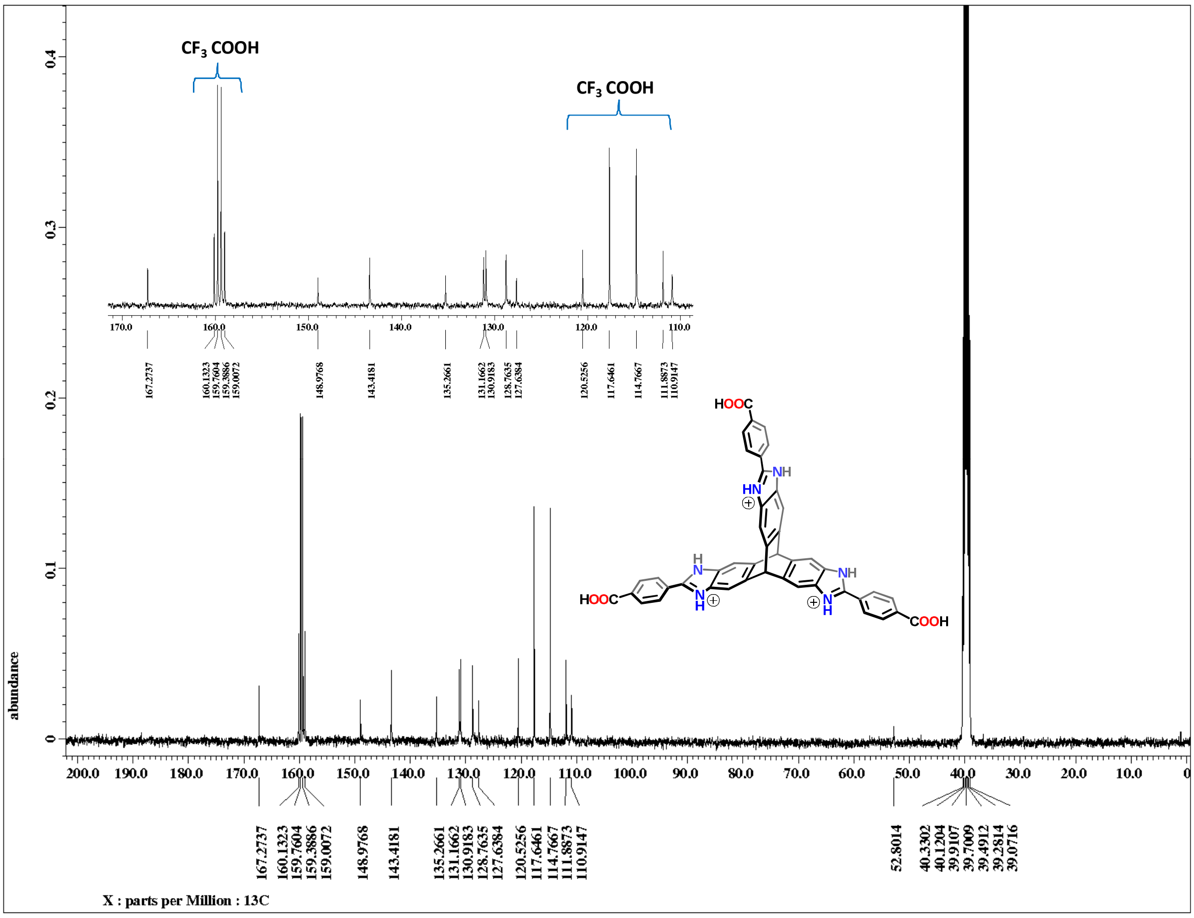

Figure S3. ^{13}C NMR (100 MHz, DMSO-d_6 + **CF_3COOH**) spectrum of **H_3TPA-3H$^+$**.

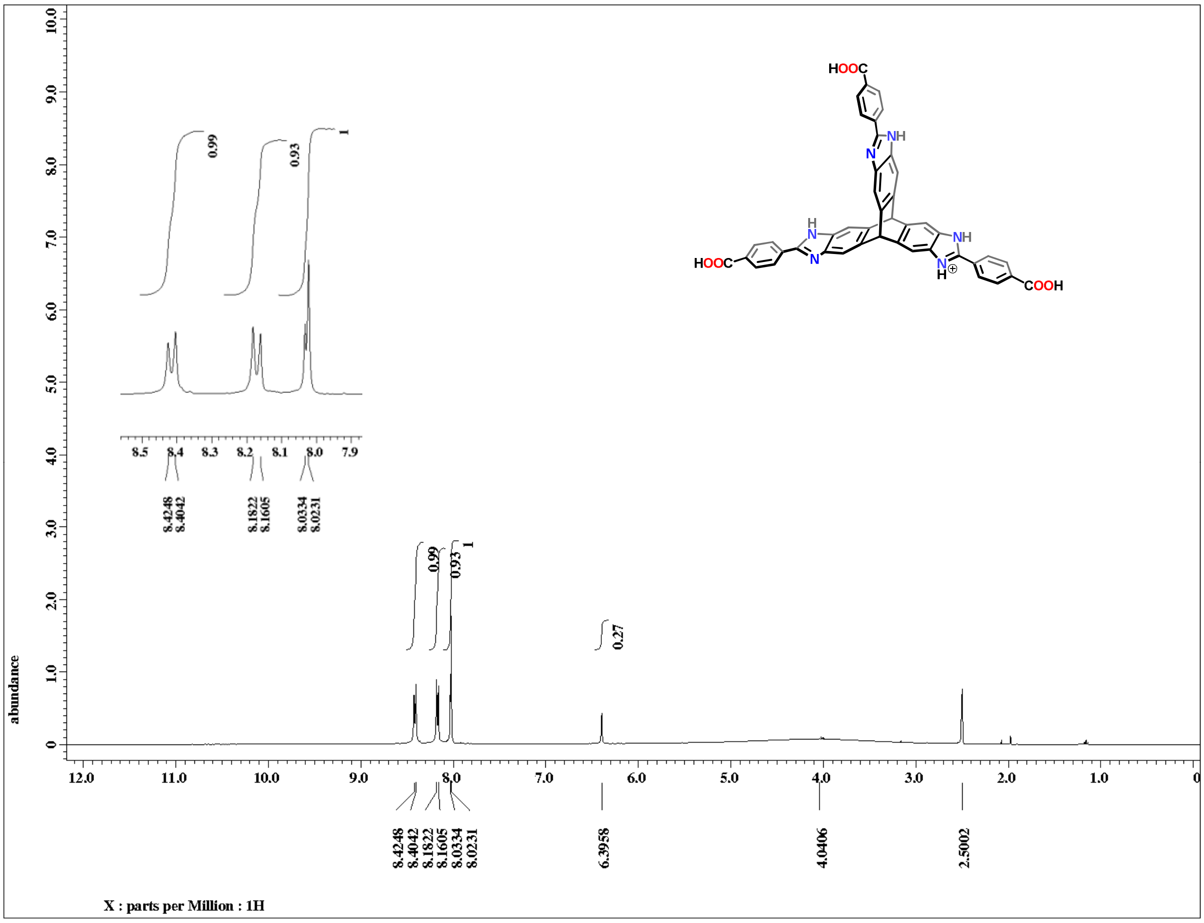

Figure S4. ^{1}H NMR (400 MHz, DMSO-d_6) spectrum of $\mathbf{H_3TPA\text{-}H^+}$.

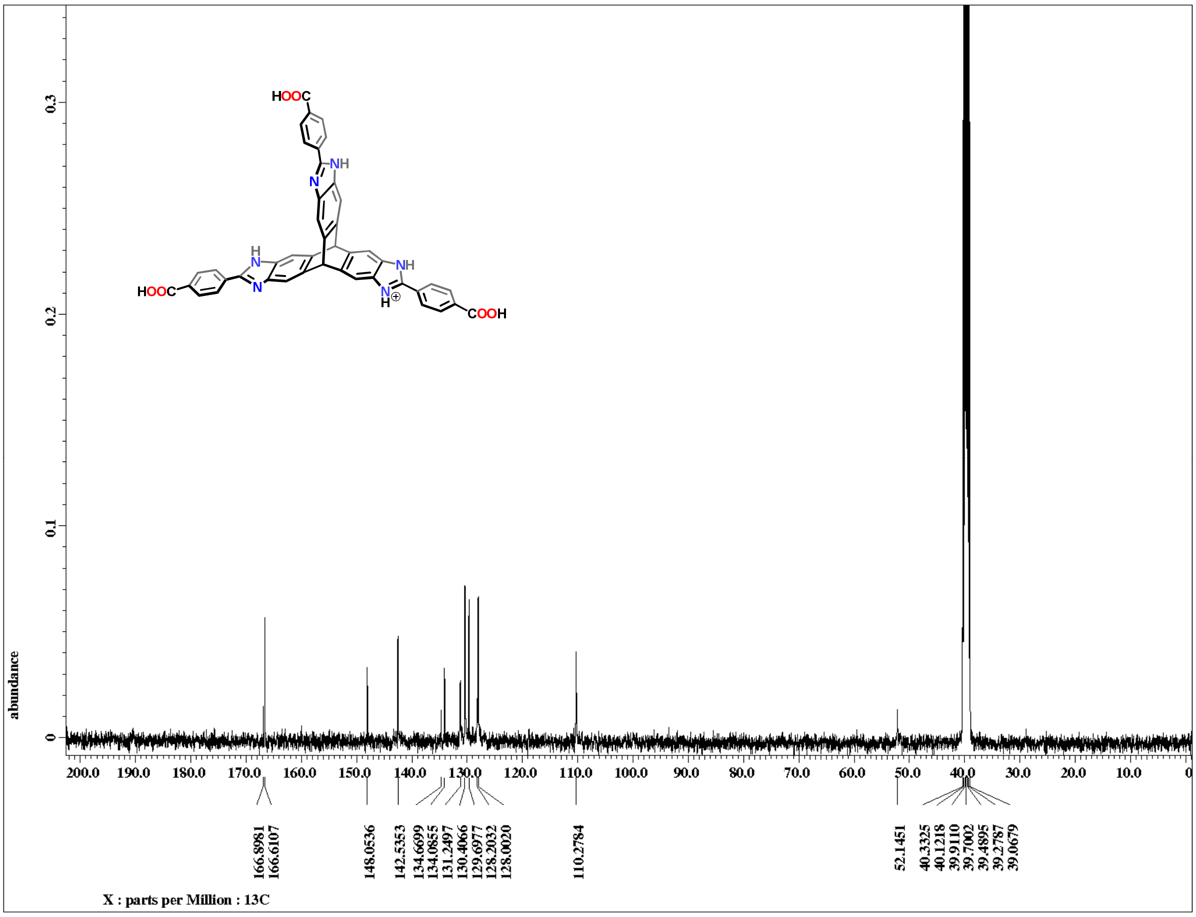

Figure S5. ^{13}C NMR (100 MHz, DMSO-d_6) spectrum of **H$_3$TPA-H$^+$**.

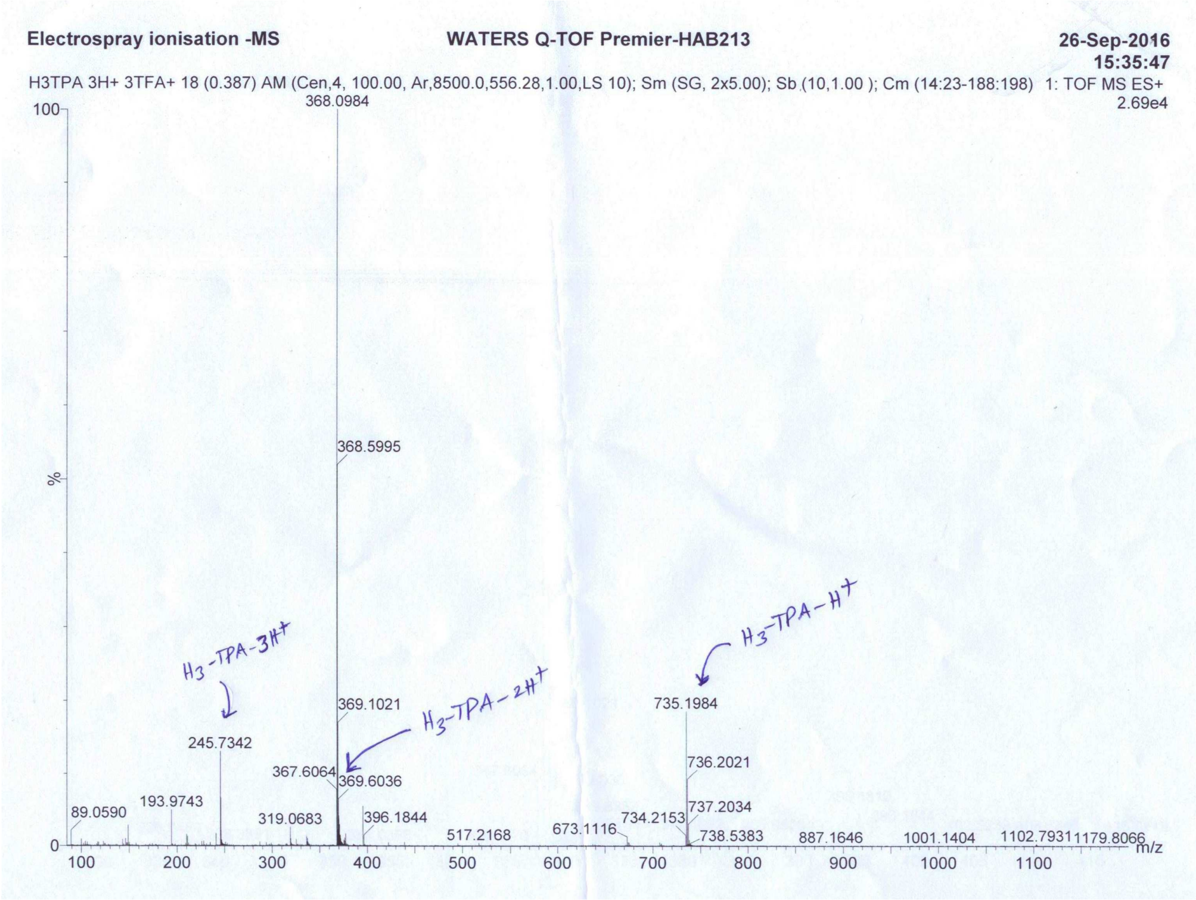

Figure S6. ESI-MS spectrum of **H_3TPA-3H$^+$**.

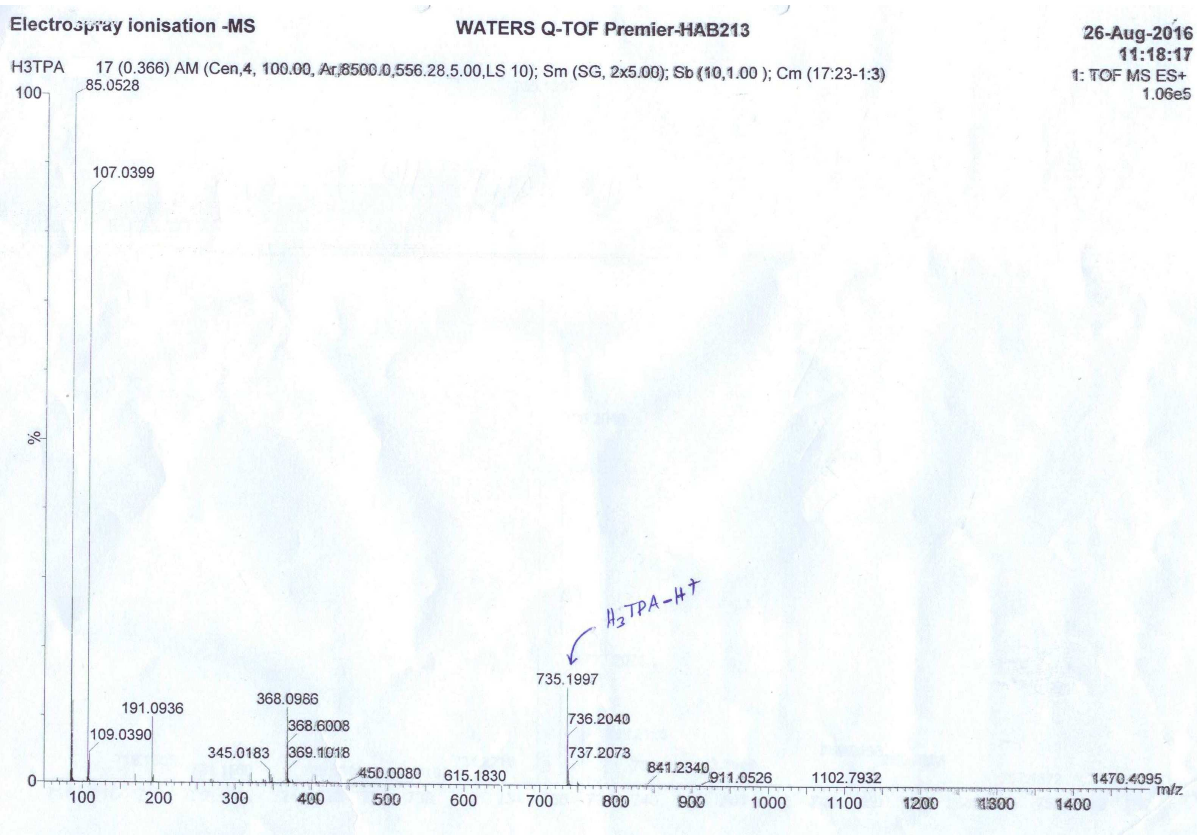

Figure S7. ESI-MS spectrum of **H_3TPA-H$^+$**.

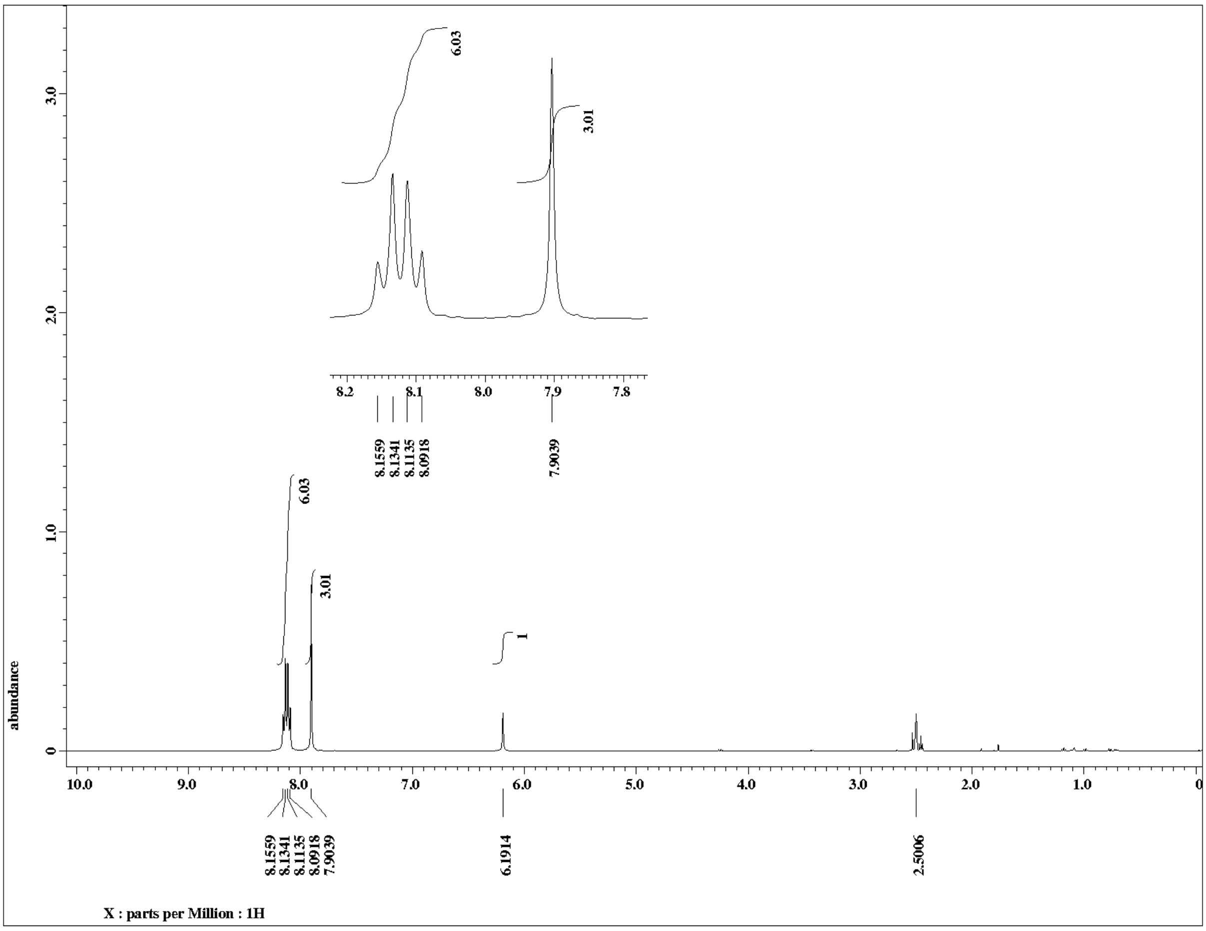

Figure S8. ^{1}H NMR (400 MHz, DMSO-d_6 + CF_3COOH (4:1, v/v)) spectrum of digested **Cd-TPA**. The MOF crystals were sonicated in the medium for 30 min.

Table S1. Crystal data and refinement parameters for **H_3TPA-3H$^+$**.

Parameters	**H_3TPA-3H$^+$**
Empirical formula	$C_{52}H_{26}F_{12}N_6O_{14}$
Formula weight	1186.79
Temperature (K)	100(2)
Wavelength (Å)	0.71073
Crystal system	Triclinic
Space group	*P*-1
a (Å)	9.425(3)
b (Å)	13.460(4)
c (Å)	24.125(8)
α (°)	92.963(7)
β (°)	91.438(8)
γ (°)	106.991(8)
Volume (Å^3)	2920.6(16)
Z	2
Calculated density (mg/m^3)	1.350
Absorption coefficient (mm^{-1})	0.124
F(000)	1200
θ range (°)	2.246 to 25.022
Index ranges	$-11 \leq h \leq 11$
	$-15 \leq k \leq 15$
	$-28 \leq l \leq 28$
Reflections collected	28908
Independent reflections	10126 [R(int) = 0.1228]
Completeness to θ = 18.942°	98.2 %
Refinement method	Full-matrix least-squares on F^2
Data/restraints/parameters	10126 / 0 / 737
Goodness-of-fit on F^2	0.965
Final R indices [I>2σ(I)]	R_1 = 0.1317, wR_2 = 0.3206
R indices (all data)	R_1 = 0.2597, wR_2 = 0.3729
Largest diff. peak and hole e.Å^{-3}	0.715 and -0.457
CCDC deposition number	1506278

Solvothermal Synthesis of Four Isostructural MOFs

To a solution of **H_3TPA-H^+** (100 mg, 0.136 mmol) in 6 mL of DMSO-DMF-H_2O (4:1:1, *v/v*) mixture, was added $Cd(NO_3)_2 \cdot 4H_2O$ (62.8 mg, 0.204 mmol). The contents were sonicated and heated in a tightly-capped glass vial at 90 °C for 2 d. The crystals of **Cd-TPA** were found to develop after cooling down to rt over 3 d, yield 82% (65 mg). The other three MOFs, namely, **Co-TPA, Mn-TPA** and **Zn-TPA** were also synthesized in a similar manner by using $CoCl_2.6H_2O$, $Mn(NO_3)_2 \cdot 6H_2O$ and $Zn(NO_3)_2 \cdot 6H_2O$, respectively. The yields were determined based on the ligand, which are 83% (50 mg) and 86% (55 mg) for **Co-** and **Mn-TPA.** Under similar solvothermal conditions, 78% **(**60 mg) of **Zn-TPA** was obtained.

To improve the intensity data set of the Cd-MOF, the solvothermal synthesis was carried out in the presence of a large excess (ca. 10 fold) of 1,4-dibromobenzene. It was anticipated that the presence of these molecules might improve the diffraction intensity due to the heavy bromine atoms. Indeed, the crystal structure was found to be isostructural with that obtained from DMSO alone, and the presence of 1,4-dibromobenzene was established in the structure, cf. vide infra.

X-Ray Crystallography

The X-ray diffraction intensity data collection for the crystals of **Cd-, Co-** and **Mn-TPA** was carried out at 100 K on a Bruker Nonius SMART APEX CCD detector system with Mo-sealed Siemens ceramic diffraction tube (λ = 0.7107 Å) and a highly oriented graphite monochromator operating at 50 kV and 30 mA. The lattice parameters and standard deviations were obtained by a least squares fit using 25 frames with 20 sec/frame exposures with the Bruker APEX2 (Version 2012.10-0) software. The data were collected in a hemisphere mode by phi and omega scans with $2\theta = 40^{o}$ and ~10 sec/frame exposures. Data processing and reduction was done using Bruker (BrukerAXSInc, Madison, Wisconsin, USA) SAINT (Version 8.27B) and empirical absorption correction made using Bruker SADABS (Version 2012/1). The structure was solved by Direct Methods using WINGX[1] and SHELXL[2] programs and refined by full matrix least-squares method based on F^2 using ShelxLe 2014 program. Hydrogens were fixed in their ideal geometries, and their contributions included in the refinement. All non-hydrogens were subjected to anisotroic refinement. The topological analysis of the crystal structure of **Cd-, Co-** and **Mn-TPA** were performed with TOPOS software.[3]

It should be noted that the diffraction intensities of Cd-MOF synthesized in the presence of DMSO were too poor, due presumably to a large void volume and dynamic solvent molecules. Further, the Cd ions were found to be disordered over two positions unlike in Mn- and Co-MOFs. Poor diffraction data led to the structure with a high of GOOF. To improve the the intensity data set, solvothermal synthesis was carried out in the presence of excess 1,4-dibromobenzene. X-ray structure determination of the crystals revealed that they are isostructural to the crystals containing DMSO. Indeed, the crystals are found to include 1,4-dibromobenzene in the lattice in lieu of DMSO. Although better diffraction intensity data set led to a better value of GOOF, the refinement did not lead to significantly improved quality of the structure, due to very high solvent-accessible volume and disorder.

We wish to mention that the intensity data and processing were carried out for as many as 16 times for the crystals of Cd-MOF, i.e., **Cd-TPA**. The disorder for the Cd ions could not be eliminated, despite all these efforts. However, for Mn- and Co-MOFs, no such disorder prevails, inspite of the fact that they are isostructural. The structures included here for the Cd-MOF are the best of 16 determinations. The crystallographic information files for **Cd-TPA (DMSO), Cd-TPA (1,4-dibromobenzene), Co-TPA** and **Mn-TPA** have been deposited at the Cambridge Crystallographic Data Centre (CCDC); the deposition numbers are 1432465 **(Cd-TPA (1,4-dibromobenzene))**, 1506926 (**Cd-TPA (DMSO)),** 1436795 **(**for **Co-TPA)** and 1436796 **(**for **Mn-TPA)**.

Table S2. Crystal data and refinement parameters for **Cd-TPA**, **Co-TPA** and **Mn-TPA**.

Parameters	**Cd-TPA (1,4-dibromobenzene)**	**Cd-TPA (DMSO)**	**Co-TPA**	**Mn-TPA**
Empirical formula	$C_{25}H_{13}N_3O_7CdBr$	$C_{24}H_{17}N_3SO_6Cd$	$C_{22}H_{11}N_3O_4Co$	$C_{22}H_{11}N_3O_6Mn$
Formula weight	659.69	587.86	440.27	468.28
Temperature (K)	100(2)	100(2)	100(2)	100(2)
Wavelength (Å)	0.71073	0.71073	0.71073	0.71073
Crystal system	Monoclinic	Monoclinic	Monoclinic	Monoclinic
Space group	*I*2/*a*	*I*2/*a*	*I*2/*a*	*I*2/*a*
a (Å)	13.9438(15)	14.0040 (14)	13.9619(16)	13.7763(11
b (Å)	42.307(6)	41.869(5)	41.194(5)	40.730(6)
c (Å)	16.9583(16)	17.1369(17)	17.1363(16)	17.9835(14)
α (°)	90	90	90	90
β (°)	104.249(7)	104.489(3)	102.485(7)	101.209(2)
γ (°)	90	90	90	90
Volume (Å^3)	9696(2)	9728.4(18)	9622.8(19)	9898.2(18)
Z	8	8	8	8
Calculated density (mg/m^3)	0.904	0.803	0.608	0.628
Absorption coefficient (mm^{-1})	1.300	0.514	0.371	0.286
F(000)	2584	2352	1784	1896
θ range (°)	2.087 to 25.172	2.094 to 18. 485	1.919 to 28.296	2.126 to 28.453
Index ranges	$-16 \le h \le 16$ $-50 \le k \le 50$ $-20 \le l \le 20$	$-12 \le h \le 12$ $-37 \le k \le 37$ $-15 \le l \le 15$	$-17 \le h \le 18$ $-54 \le k \le 54$ $-22 \le l \le 22$	$-18 \le h \le 18$ $-54 \le k \le 54$ $-24 \le l \le 24$
Reflections collected	78947	30948	42934	75845
Independent reflections	8696 [R(int) = 0.0575]	3617 [R(int) = 0.0345]	11928 [R(int) = 0.0724]	12462 [R(int) = 0.1160]
Completeness to θ = 18.942°	99.7 %	99.6 %	99.9 %	99.9 %
Refinement method	Full-matrix least-squares on F^2	Full-matrix least-squares on F^2	Full-matrix least-squares on F^2	Full-matrix least-squares on F^2
Data/restraints/parameters	8696 / 0 / 335	3617 / 0 / 306	11928 / 0 / 273	12462 / 0 / 291
Goodness-of-fit on F^2	1.840	2.383	1.230	0.958
Final R indices [I>2σ(I)]	R_1 = 0.1802, wR_2 = 0.4784	R_1 = 0.1699, wR_2 = 0.4741	R_1 = 0.1388, wR_2 = 0.3957	R_1 = 0.1177, wR_2 = 0.3329
R indices (all data)	R_1 = 0.2267, wR_2 = 0.5026	R_1 = 0.1801, wR_2 = 0.4914	R_1 = 0.2324, wR_2 = 0.4319	R_1 = 0.3694, wR_2 = 0.4213
Largest diff. peak and hole e.Å^{-3}	1.726 and -1.664	1.092 and -1.076	2.500 and -0.780	0.457 and -0.339
CCDC deposition number	1432465	1506926	1436795	1436796

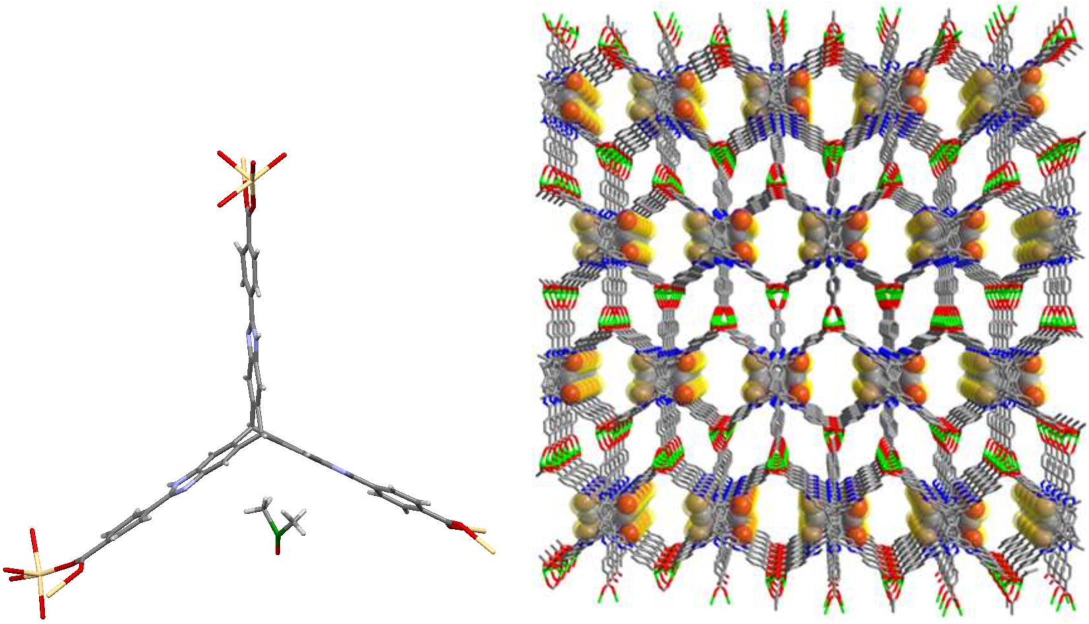

Figure S9. Perspective view of the molecular structure with DMSO (left) and crystal packing (right) of **Cd-TPA (DMSO)** down a-axis; the guest DMSO molecules are shown in space-filling model.

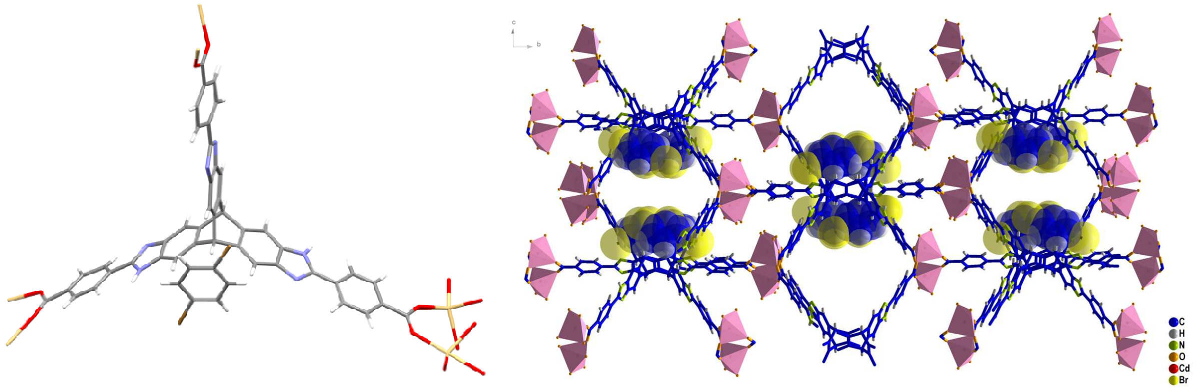

Figure S10. Perspective view of the molecular structure with 1,4-dibromobenzene (left) and crystal packing (right) of **Cd-TPA (1,4-dibromobenzene)** down a-axis; the guest 1,4-dibromobenzene molecules are shown in space-filling model.

Topographical Representation

In Figure S11 is shown a simplified topological representation of the network of the four isostructural MOFs (**Cd-TPA** as representative case). As revealed by ToposPro program, the 2D-network of **Cd-TPA** is honeycomb (hcb) with the (3-c) nets in (1 0 1) planes. The overall 3D framework of **Cd-TPA** was found to be “gra” type, as the honeycomb layers are interconnected by N-H···N hydrogen bonds such that the overall topology is a 3,5-coordinated 2-nodal net with a point symbol $\{6^3\}\{6^9.8\}$ with nodes stoichiometry (3-c)(5-c). This is based on the consideration that the 3-connecting nodes are related to the centeriod of bimetallic-SBU cluster and 5-connecting nodes are related to the centroid of organic linker.

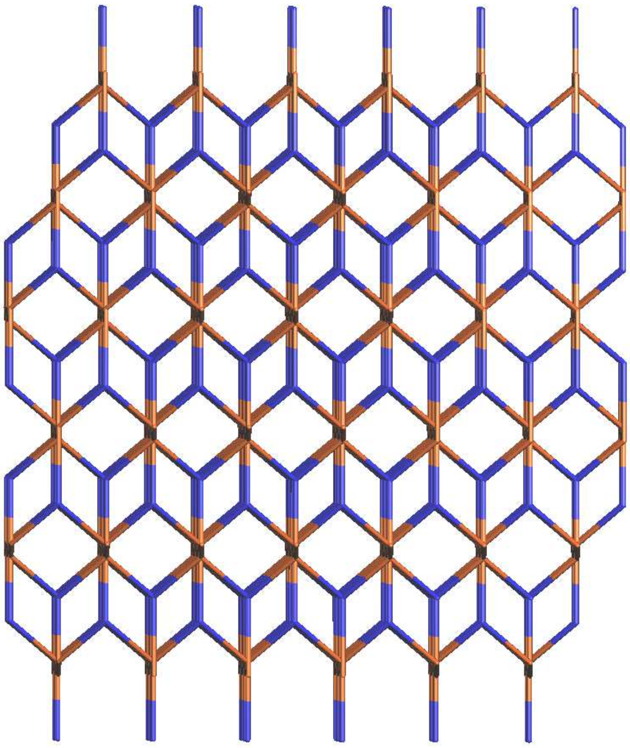

Figure S11. Simplified topological network of **Cd-TPA**.

References.

1. L. J. Farrugia, *J. Appl. Cryst.*, 2012, **45**, 849–854.

2. G. M. Sheldrick, *Acta Cryst.*, 2008, **A64**, 112–122.

3. V. A. Blatov, A. P. Shevchenko, V. N. Serezhkin, *J. Appl. Cryst.* 2000, **33**, 1193.

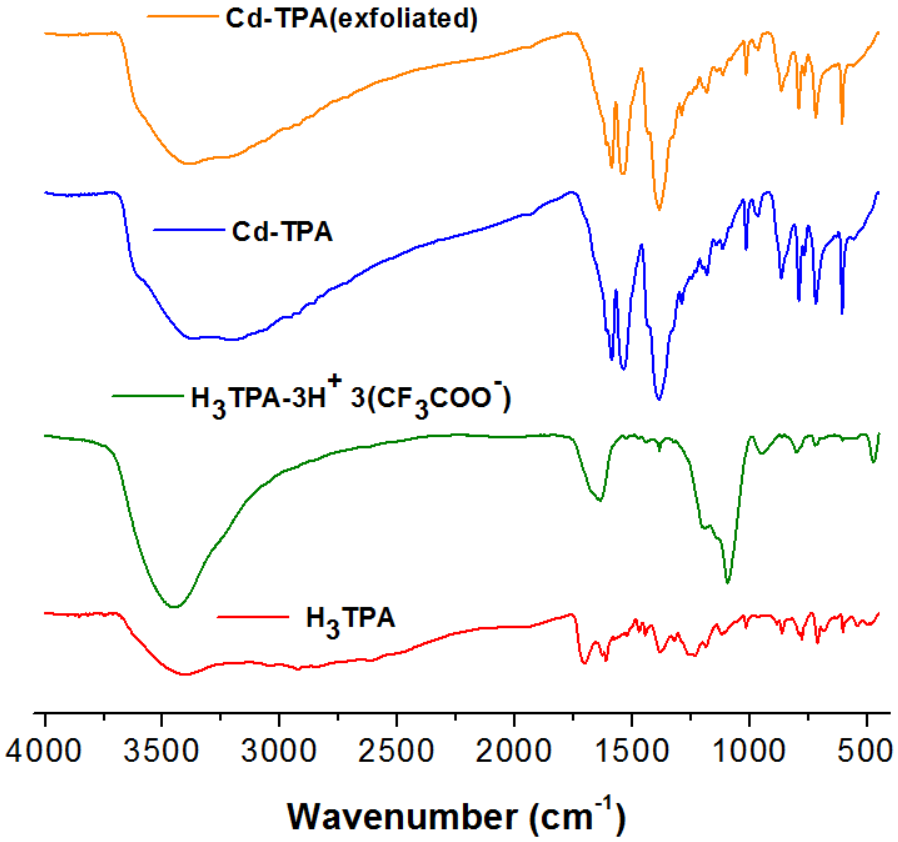

Figure S12. IR (KBr) spectra of **H_3TPA, H_3TPA-3H$^+$ 3CF$_3$COO$^-$, Cd-TPA** and **Cd-TPA** (exfoliated).

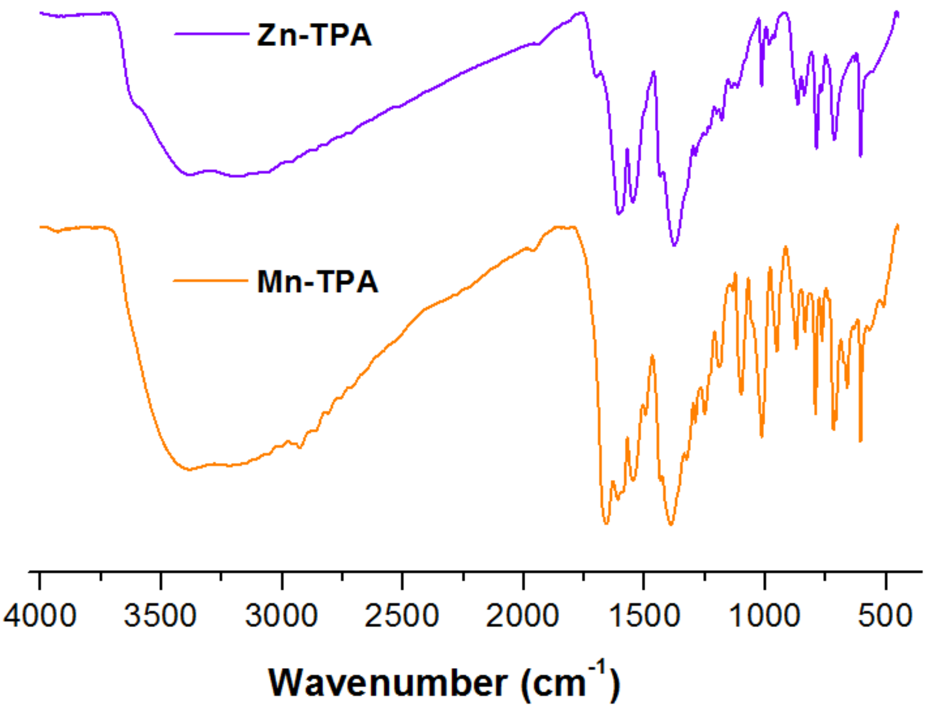

Figure S13. IR (KBr) spectra of **Mn-TPA** and **Zn-TPA**.

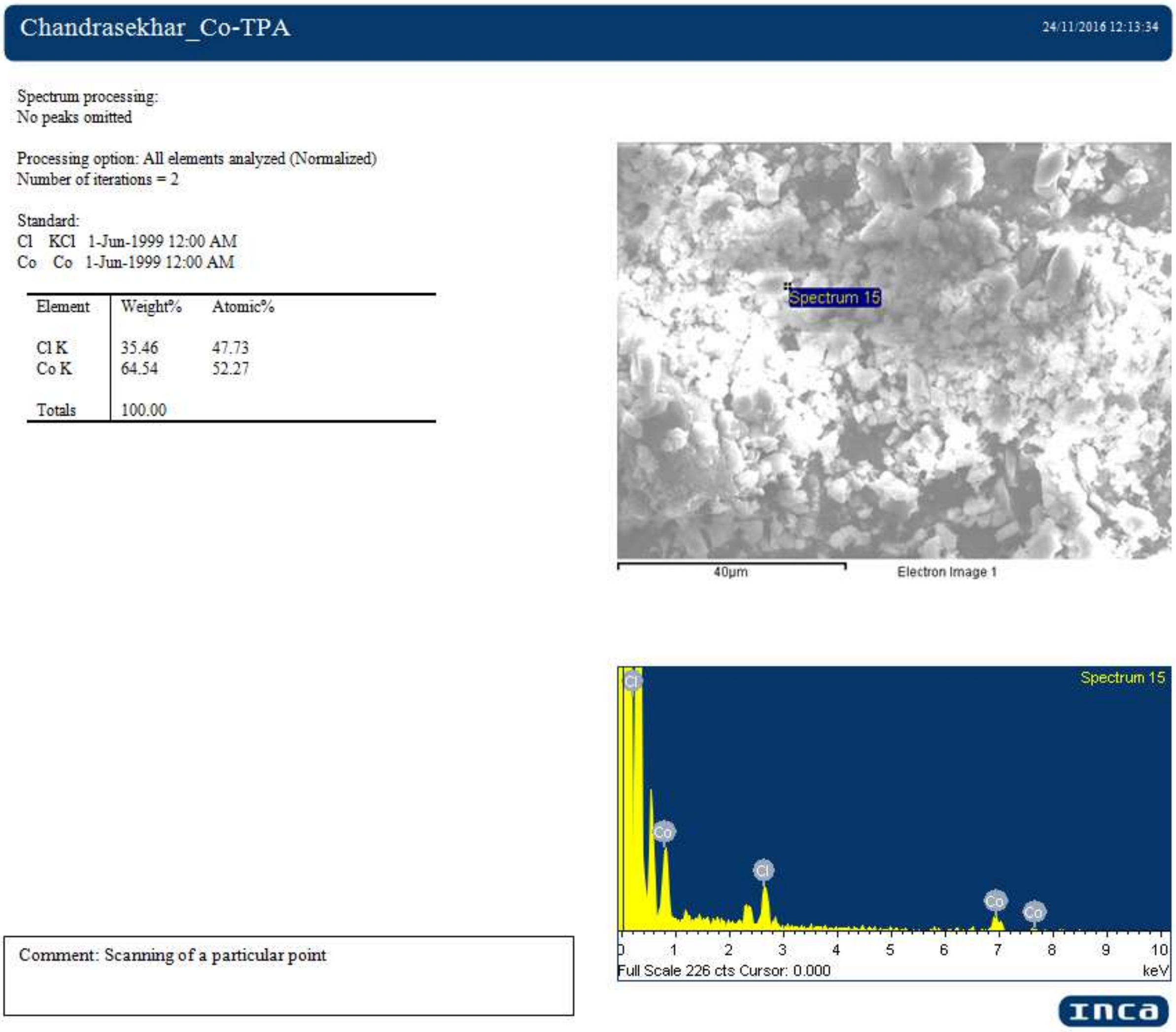

Chandrasekhar_Co-TPA

24/11/2016 12:13:34

Spectrum processing:
No peaks omitted

Processing option: All elements analyzed (Normalized)
Number of iterations = 2

Standard:
Cl KCl 1-Jun-1999 12:00 AM
Co Co 1-Jun-1999 12:00 AM

Element	Weight%	Atomic%
Cl K	35.46	47.73
Co K	64.54	52.27
Totals	100.00	

Comment: Scanning of a particular point

Figure S14. SEM-EDX analysis of **Co-TPA**. Notice the presence of chlorine content.

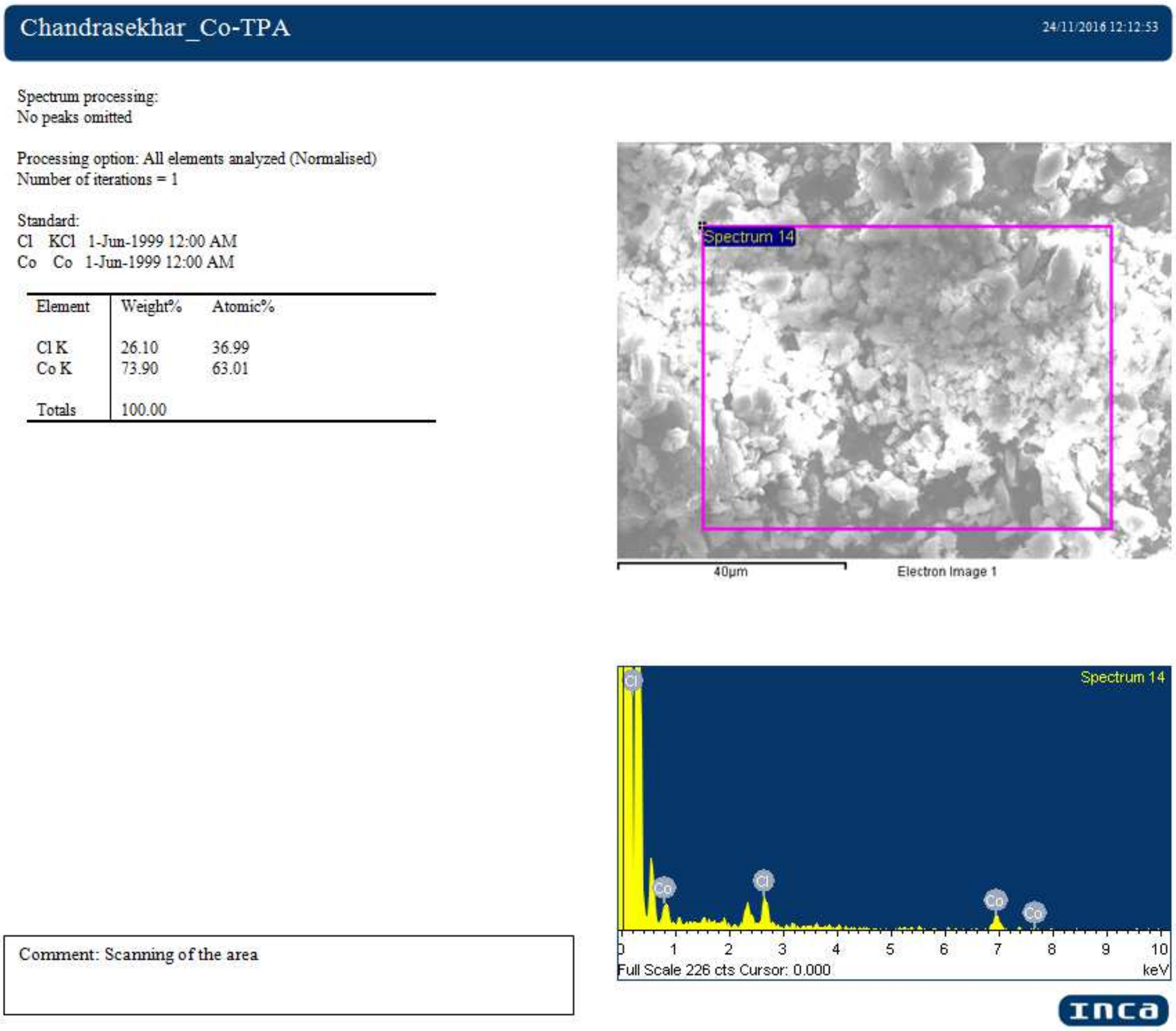

Chandrasekhar_Co-TPA

24/11/2016 12:12:53

Spectrum processing:
No peaks omitted

Processing option: All elements analyzed (Normalised)
Number of iterations = 1

Standard:
Cl KCl 1-Jun-1999 12:00 AM
Co Co 1-Jun-1999 12:00 AM

Element	Weight%	Atomic%
Cl K	26.10	36.99
Co K	73.90	63.01
Totals	100.00	

Comment: Scanning of the area

Figure S15. SEM-EDX analysis of **Co-TPA**. Notice the presence of chlorine content.

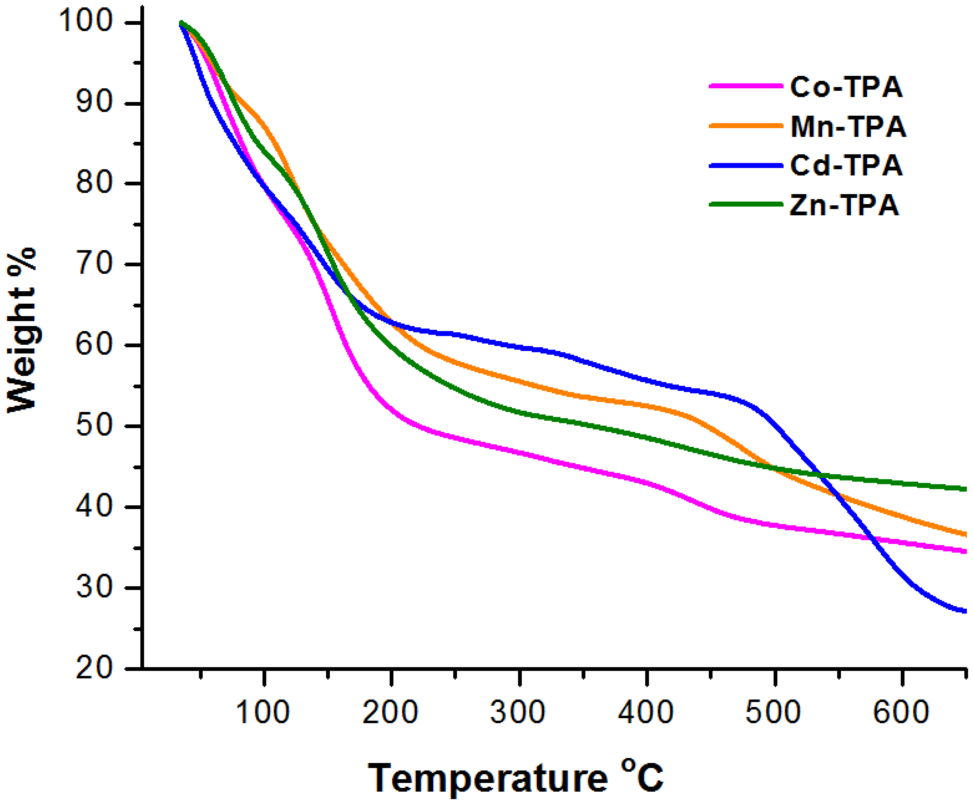

Figure S16. TGA profiles of **Co-**, **Mn-**, **Cd-** and **Zn-TPA**.

Gas Adsorption Studies

Activation of MOFs. All the MOFs were activated prior to the gas adsorption studies by solvent exchange followed by thermal activation. The crystals of the MOFs were soaked in acetone/DCM (1:1, *v/v*) for 1 d, and then in DCM for another 1 d. In each case, the supernatant solvent was replaced by a fresh solvent regularly at an interval of 3 h. The solvent-exchanged sample was dried under vacuum at room temperature for 6 h. Prior to gas sorption experiments, thermal activation at a temperature of 50 °C under ultrahigh vacuum was performed for 6 h to remove any trace amount of solvent present in the MOFs.

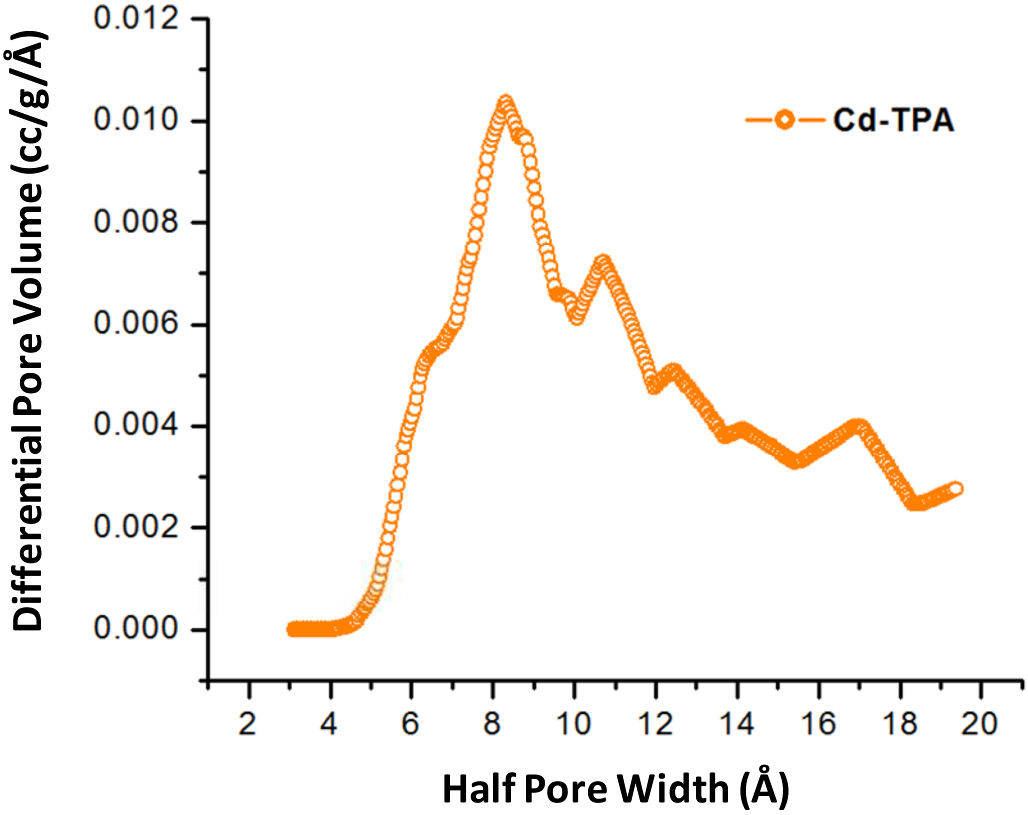

Figure S17. Pore size distribution for **Cd-TPA**.

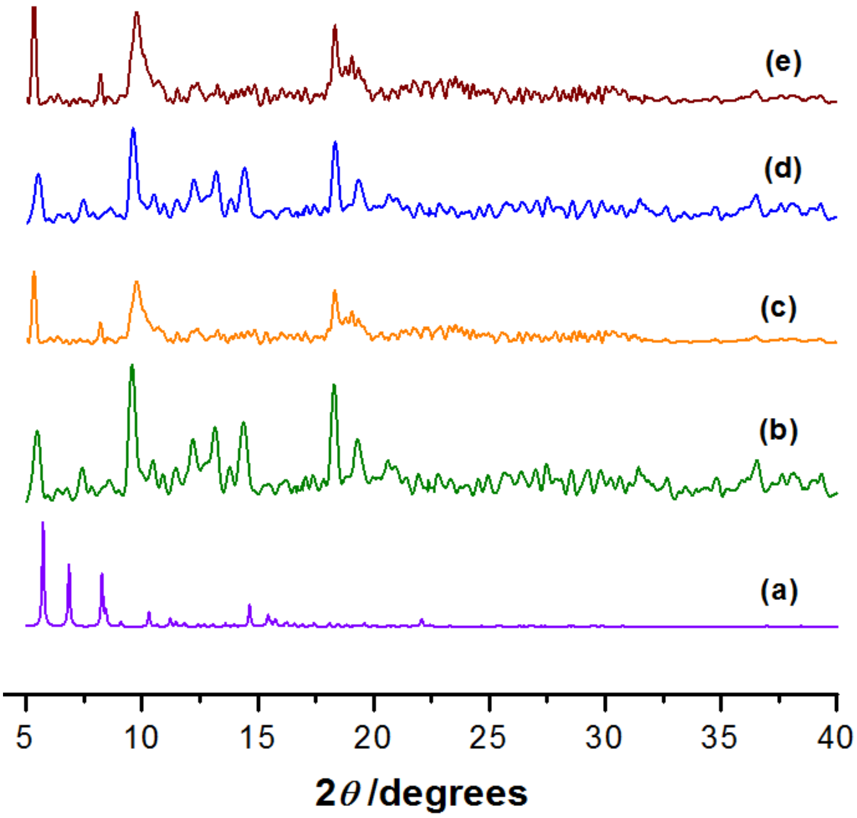

Figure S18. PXRD profiles of (a) simulated **Cd-TPA**, (b) **Cd-TPA** after activation, (c) **Mn-TPA** after activation, (d) **Zn-TPA** after activation and (e) **Co-TPA** after activation. The PXRDs were found to be unaffected after gas adsorption/desorption.

Determination of Selectivity Factors for CO_2 vs. N_2 Adsorption

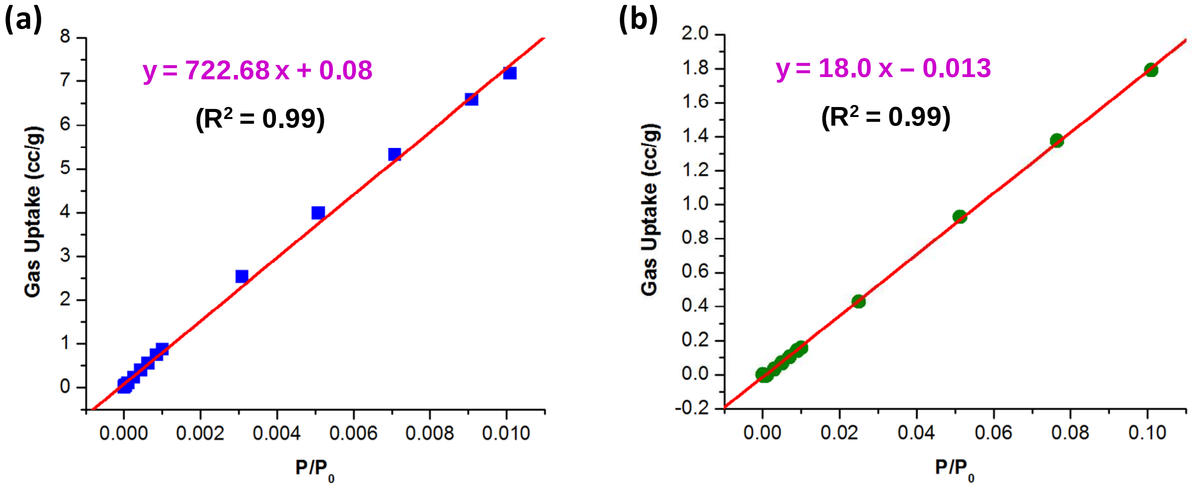

Figure S19. Initial slope calculation for CO_2 (a) and N_2 (b) isotherms for **Co-TPA** at 273 K. The calculated CO_2/N_2 selectivity is 722.68:18.0, i.e., 40:1 at 273 K.

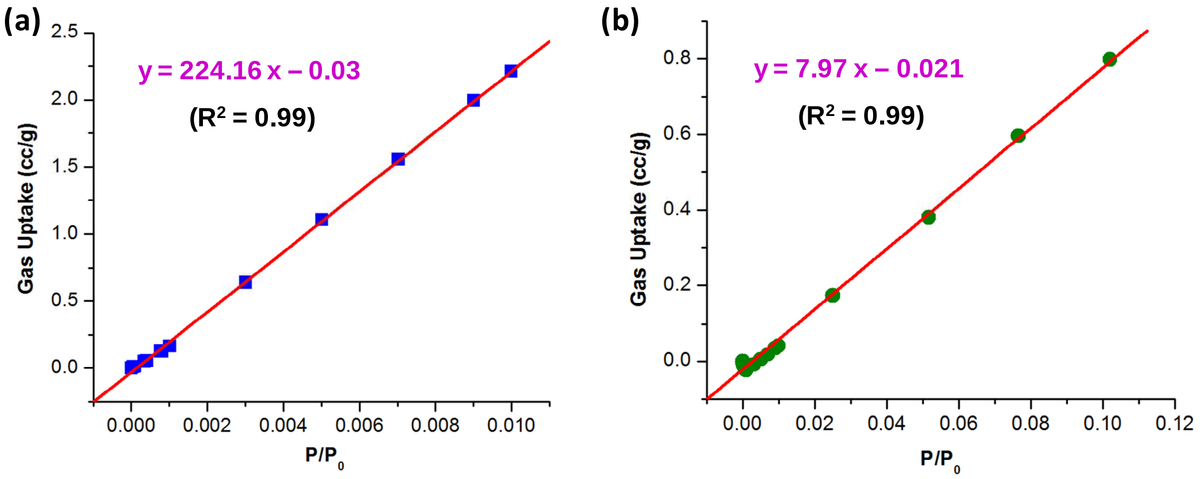

Figure S20. Initial slope calculation for CO_2 (a) and N_2 (b) isotherms for **Co-TPA** at 298 K. The calculated CO_2/N_2 selectivity is 224.16:7.97, i.e., 28:1 at 298 K.

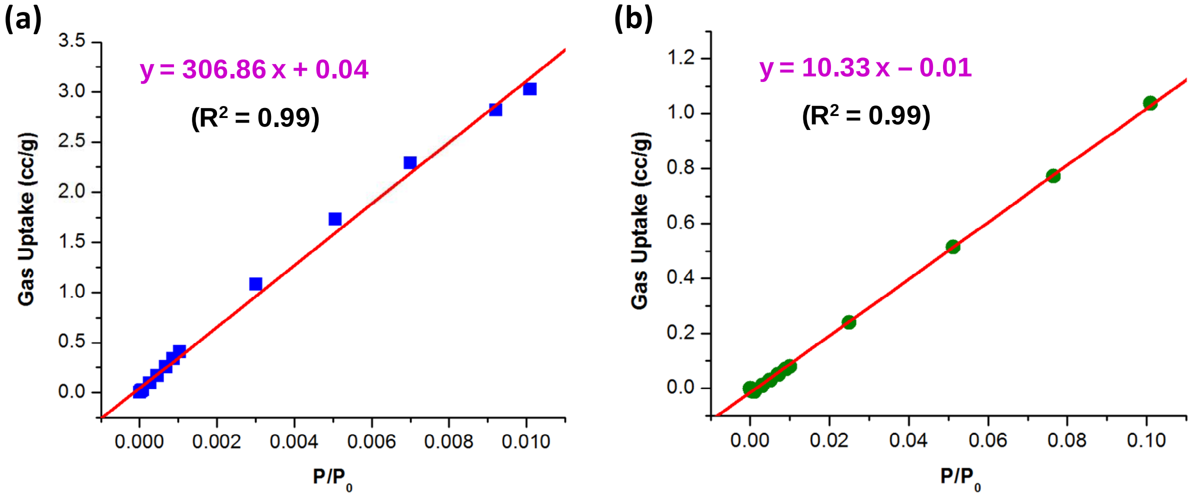

Figure S21. Initial slope calculation for CO_2 (a) and N_2 (b) isotherms for **Mn-TPA** at 273 K. The calculated CO_2/N_2 selectivity is 306.86:10.33, i.e., 30:1 at 273 K.

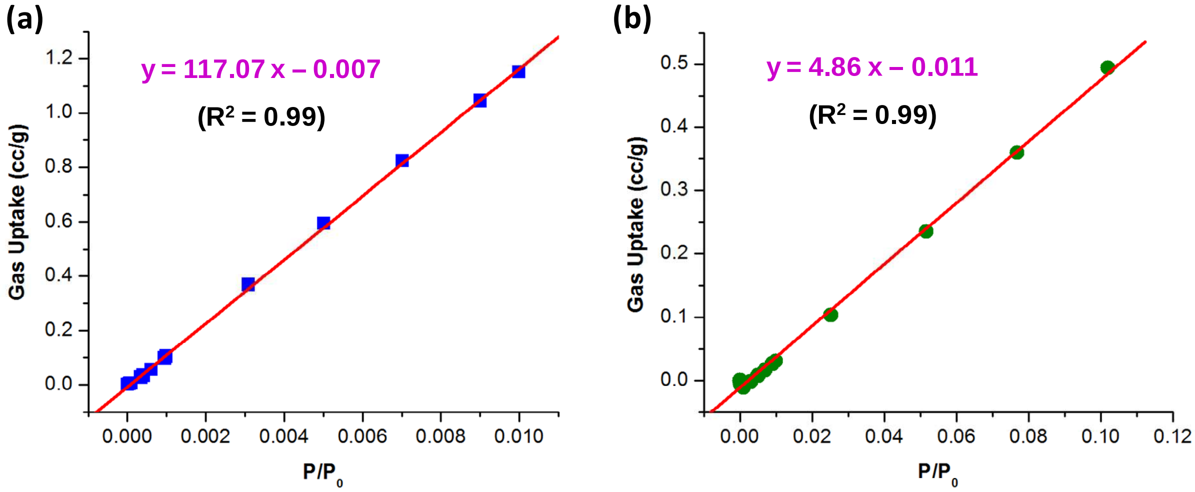

Figure S22. Initial slope calculation for CO_2 (a) and N_2 (b) isotherms for **Mn-TPA** at 298 K. The calculated CO_2/N_2 selectivity is 117.07:4.86, i.e., 24:1 at 298 K.

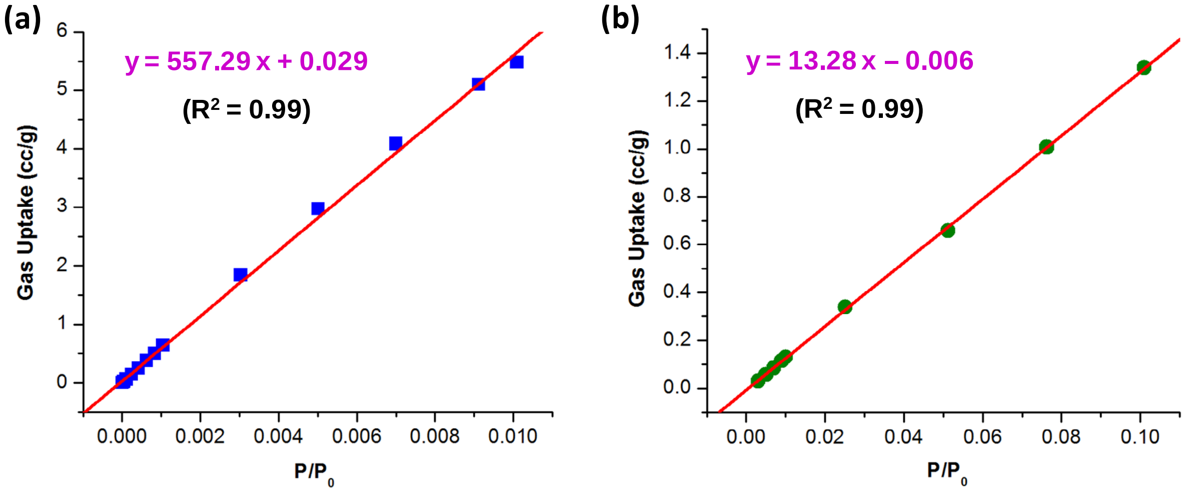

Figure S23. Initial slope calculation for CO_2 (a) and N_2 (b) isotherms for **Cd-TPA** at 273 K. The calculated CO_2/N_2 selectivity is 557.29:13.28, i.e., 42:1 at 273 K.

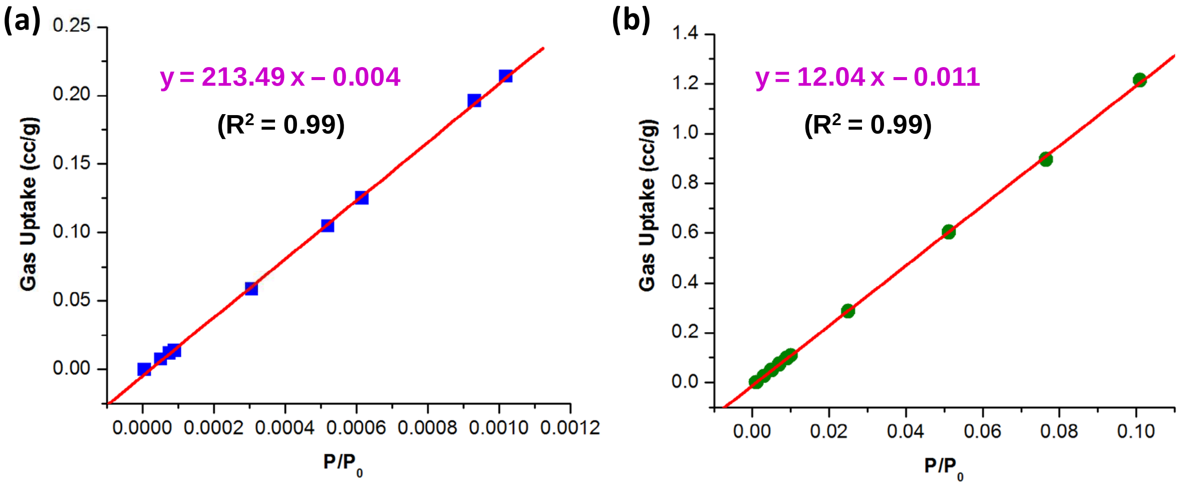

Figure S24. Initial slope calculation for CO_2 (a) and N_2 (b) isotherms for **Cd-TPA** at 298 K. The calculated CO_2/N_2 selectivity is 213.49:12.04, i.e., 18:1 at 298 K.

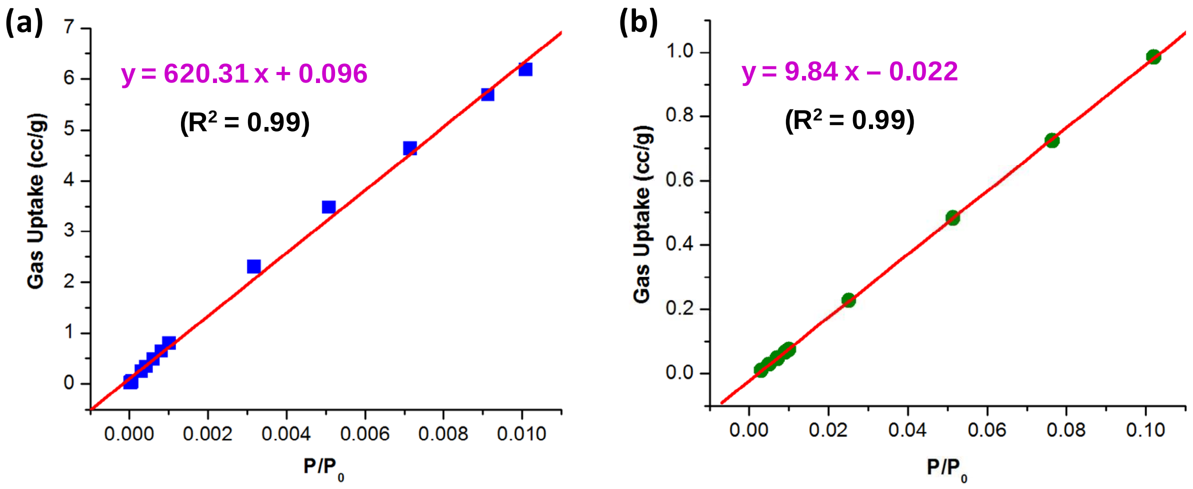

Figure S25. Initial slope calculation for CO_2 (a) and N_2 (b) isotherms for **Zn-TPA** at 273 K. The calculated CO_2/N_2 selectivity is 620.31:9.84, i.e., 63:1 at 273 K.

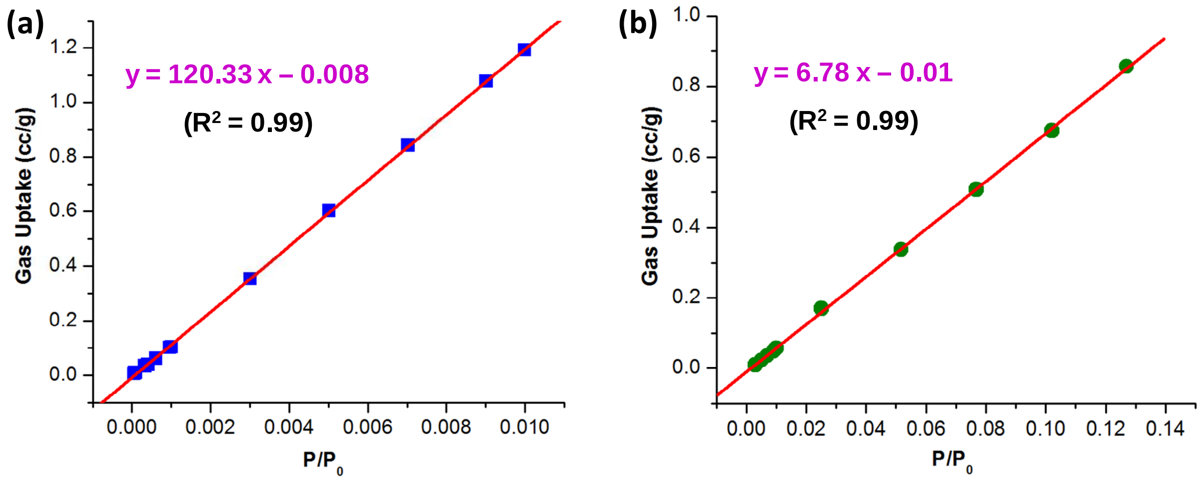

Figure S26. Initial slope calculation for CO_2 (a) and N_2 (b) isotherms for **Zn-TPA** at 298 K. The calculated CO_2/N_2 selectivity is 120.33:6.78, i.e., 18:1 at 298 K.

Steady-State Fluorescence Spectroscopy

All the steady-state fluorescence measurements were performed at 298 K on a FluoroMax-4: FM4-3000 spectrofluorometer (Horiba Jobin Yvon Technology), which was standardized with an R928 photomultiplier tube, a DM302 photon-counting acquisition module biased at 950 V, a 1200 lines/mm grating blazed at 330 nm in the excitation monochromator and a 1200 lines/mm grating blazed at 500 nm in the emission monochromator. The slit widths for both excitation and emission were fixed at 1.0 nm band pass and the accuracy in measuring the wavelength was ±1.0 nm. The fluorescence quantum yield determinations for the colloidal solutions of **Cd-TPA** were performed by using a 'Quanta-φ: F-3029' Horiba Scientific integrating sphere (sphere inner diameter: 150 mm) connected to the spectrofluorimeter.

Photophysical Properties of H_3TPA. In Figure S27, are shown the absorption and fluorescence emission spectra of **H_3TPA** (5 μM) in a polar protic solvent such as ethanol and a polar aprotic solvent such as DMSO. The absorption spectra are characterized by the presence of strong bands with high molar absorptivity in the region between 320–400 nm which corresponds to π–π^* transition; the absorption spectra are found to taper off at ca. 425 nm. Interestingly, the absorption maximum in the case of DMSO (355 nm) was found to be bathochromically-shifted by ca. 10 nm when compared to that observed with ethanol (345 nm), Table S3.

Insofar as the emission properties are concerned, **H_3TPA** was found to be virtually non-fluorescent in the solid-state. However, moderate fluorescence emission was observed for the latter in solutions of ethanol and DMSO. A considerable difference in the fluorescence property of **H_3TPA** in the two different solvents is noteworthy. For instance, the emission maximum was found to have a significant bathochromic shift of ca. 45 nm on going from ethanol (410 nm) to DMSO (455 nm). In fact, one notices considerably higher Stokes shift of ca. 100 nm in DMSO when compared to that observed in ethanol (65 nm). As shown in Table S3, **H_3TPA** was found to exhibit a fluorescence quantum yields of ca. 6.3% in ethanol, whereas the same was found to be 18.2% in DMSO. Furthermore, time-resolved fluorescence measurements reveal that the singlet lifetime of **H_3TPA** in DMSO (2.25 ns) is ca. 2.4 fold higher than that observed in ethanol (0.93 ns). Thus, one may readily understand that the non-radiative rate constant (k_{nr}) in ethanol (10.1×10^8 s^{-1}) is higher than that calculated for DMSO (3.6×10^8 s^{-1}). Evidently, the nature of solvent plays a decisive role in modulating the stability of the excited-state of **H$_3$TPA** such that the fluorescence properties in DMSO are much enhanced than those observed with ethanol.

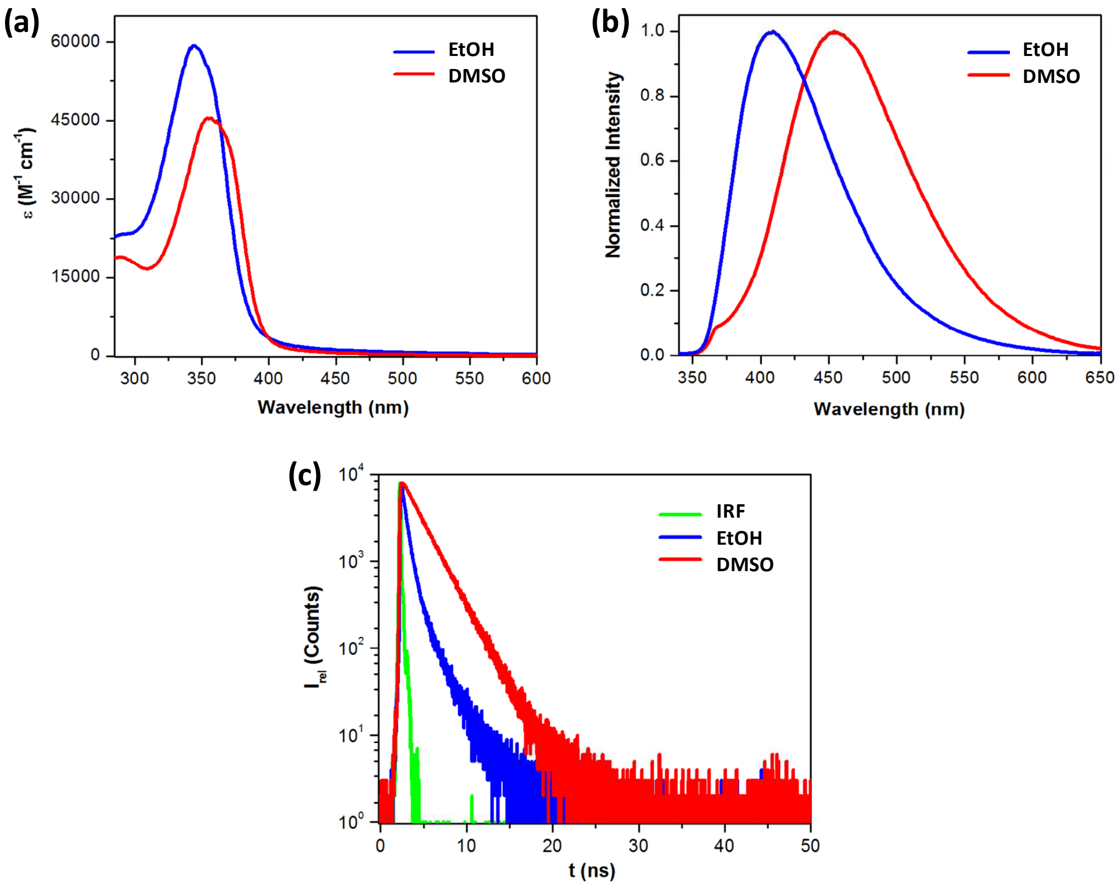

Figure S27. (a) UV-vis. absorption spectra, (b) fluorescence emission spectra and (c) fluorescence lifetime decay traces of **H$_3$TPA** (5 μM) in ethanol and DMSO.

Table S3. Photophysical Properties of **H_3TPA**.

photophysical properties		solvents	
		EtOH	DMSO
absorption	λ_{max} (nm) [a]	345	355
	ε (M^{-1} cm^{-1}) [b]	59350	45350
fluorescence emission	λ_{max} (nm) [a]	410	455
	E_S (kcal/mol) [c]	69.73	62.84
	Stokes shift (nm) [d]	65	100
	Φ_f (%) [e]	6.3	18.2
	τ_f (ns) [f]	0.93 [g]	2.25 [h]
	k_r (10^7 s^{-1}) [i]	6.8	8.1
	k_{nr} (10^8 s^{-1}) [i]	10.1	3.6

[a] Accuracy of the values of λ_{max} for both UV-vis absorption and fluorescence are ± 1 nm. [b] ε refers to molar extinction coefficient. [c] E_S refers to singlet excitation energy as determined from the fluorescence maximum. [d] Estimated from the difference of λ_{max} between absorption and fluorescence spectra. [e] Fluorescence quantum yields (Φ_f) were determined using quinine sulfate in 0.5 M H_2SO_4 as the standard (λ_{exc} = 330 nm). [f] Fluorescence lifetime (τ_f) in each case was determined for the decay monitored at the emission maximum (λ_{exc} = 375 nm). The decay in each case was fitted to a biexponential function. [g] The two components were: τ_1 = 0.60 ns (α_1 = 0.76) and τ_2 = 1.99 ns (α_2 = 0.24). [h] The two components were: τ_1 = 0.87 ns (α_1 = 0.03) and τ_2 = 2.30 ns (α_2 = 0.97). [i] k_r and k_{nr} refer to radiative and non-radiative rate constant respectively.

Ultrasound-Induced Liquid-Phase Exfoliation (UILPE) and Solvent-Induced Fluorescence Studies of Exfoliated 2D Material. Ultrasonication of **Cd-TPA** in various solvents was carried out using a BANDELIN SONOREX ultrasonicator bath (25 kHz). In a typical process, the activated crystals of **Cd-TPA** were dispersed and then ultrasonicated in various solvents (0.1 mg/mL) for 20 min at 298 K to give rise to homogeneous colloidal solutions, which were further filtered through a Whatman filter paper. These colloidal solutions were subsequently placed in a quartz cell of 1 cm width for fluorescence spectral acquisition (λ_{exc} = 330 nm). The slit widths for both excitation and emission were fixed at 1.0 nm bandpass and the accuracy in measuring the wavelength was ±1.0 nm.

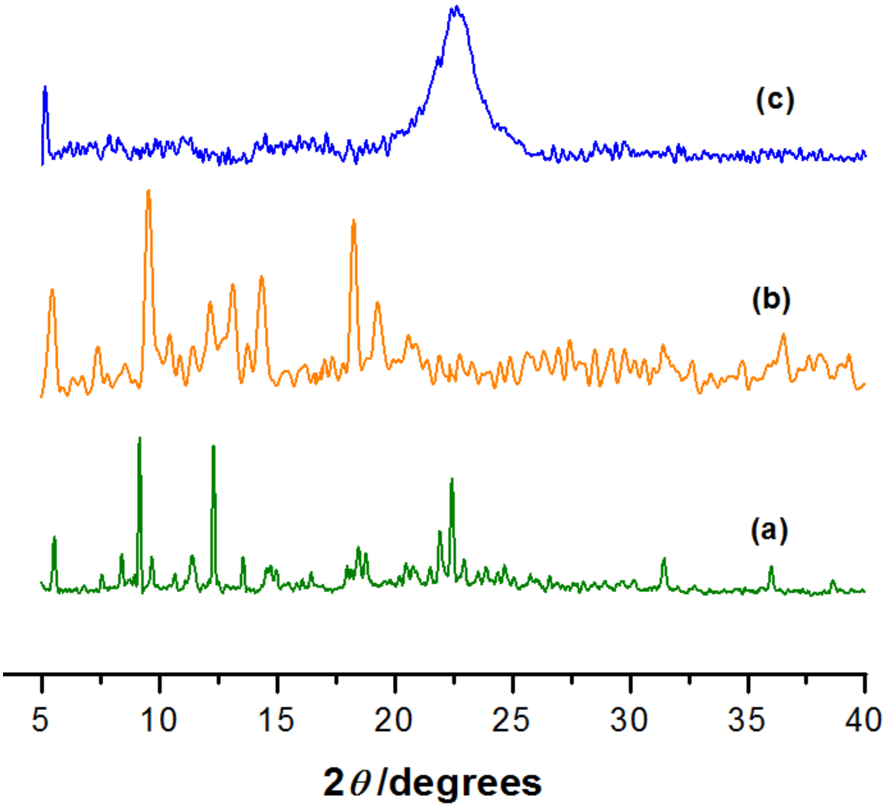

Figure S28. PXRD profiles of (a) pristine **Cd-TPA**, (b) **Cd-TPA** after activation and (c) the solid material obtained after exfoliation of **Cd-TPA** in EtOH.

AFM Analysis of Exfoliated Cd-TPA Nanosheets. The ethanolic colloidal suspension of **Cd-TPA** (0.1 mg/mL) was adsorbed on a silicon wafer by drop casting (10 μL) and air dried. Subsequently, the morphology of the surface was analyzed by atomic force microscopy (AFM) using an Asylum Research system (Model Number: AC240TS-R3, Oxford Instruments Company). The AFM images were recorded in the dynamic mode (i.e., tapping or non-contact mode) using a silicon tip (radius = 9 ± 2 nm) and a silicon cantilever (with Al (100) coating) with a resonance frequency (f) of 70 kHz and a force constant (k) of 2 N/m. The operations were carried out at room temperature under ambient air conditions. The images were processed using the Asylum Research system software provided with the AFM instrument.

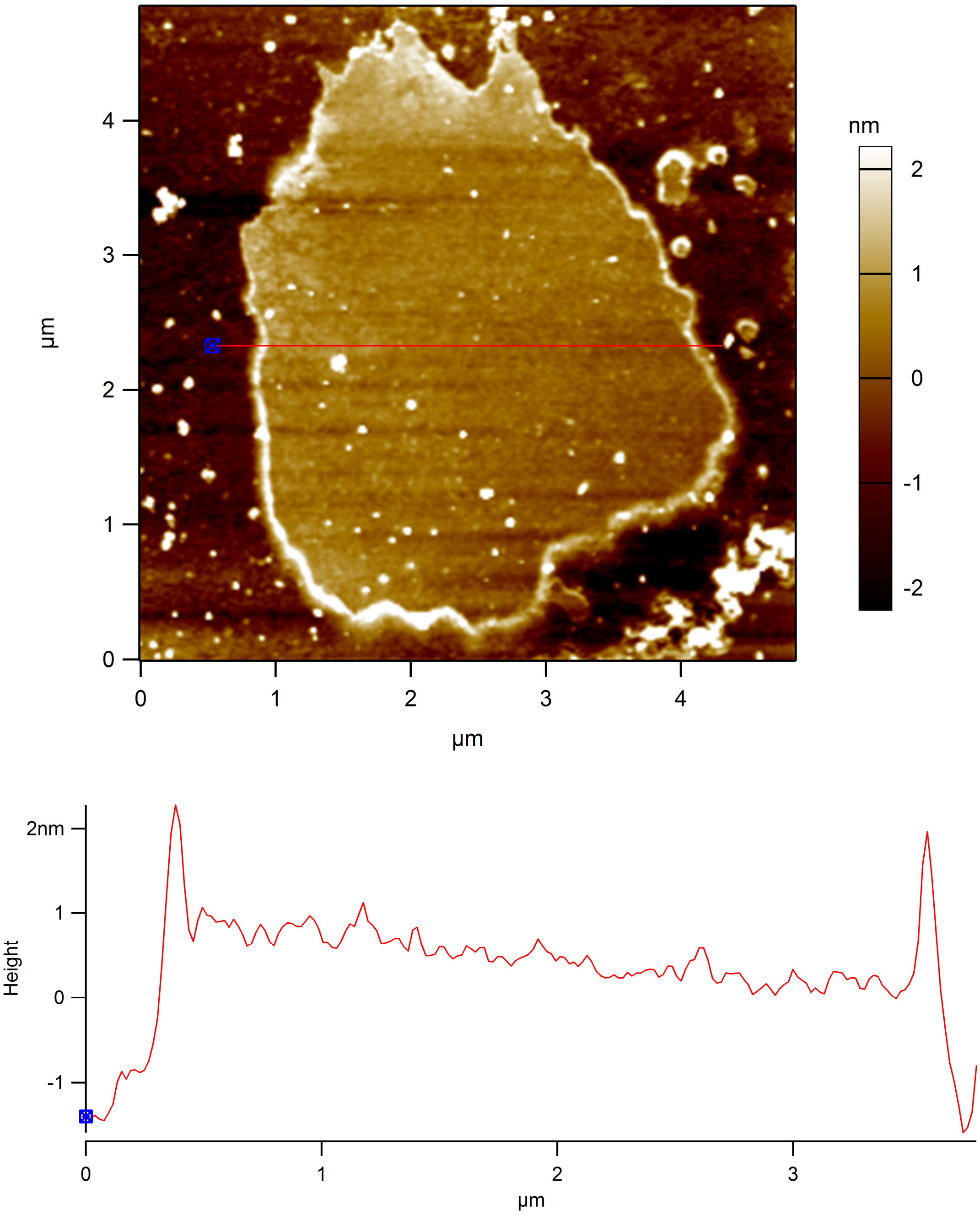

Figure S29. AFM image (a) and height profile diagram for the exfoliated 2D layers of **Cd-TPA**. Notice the presence of flat 2D flaky material.

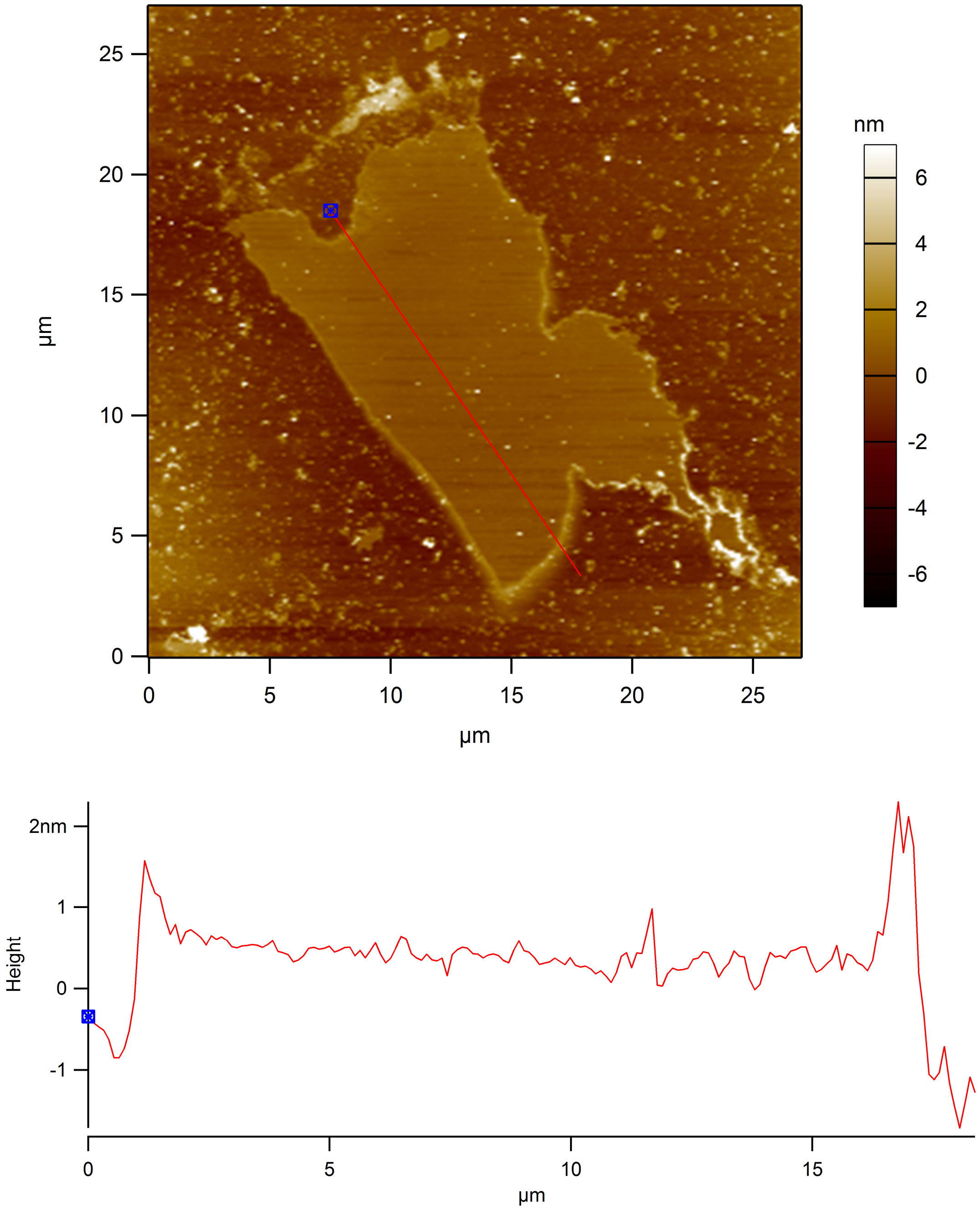

Figure S30. AFM image (a) and height profile diagram for the exfoliated 2D layers of **Cd-TPA**. Notice the presence of flat 2D sheet-like structure.

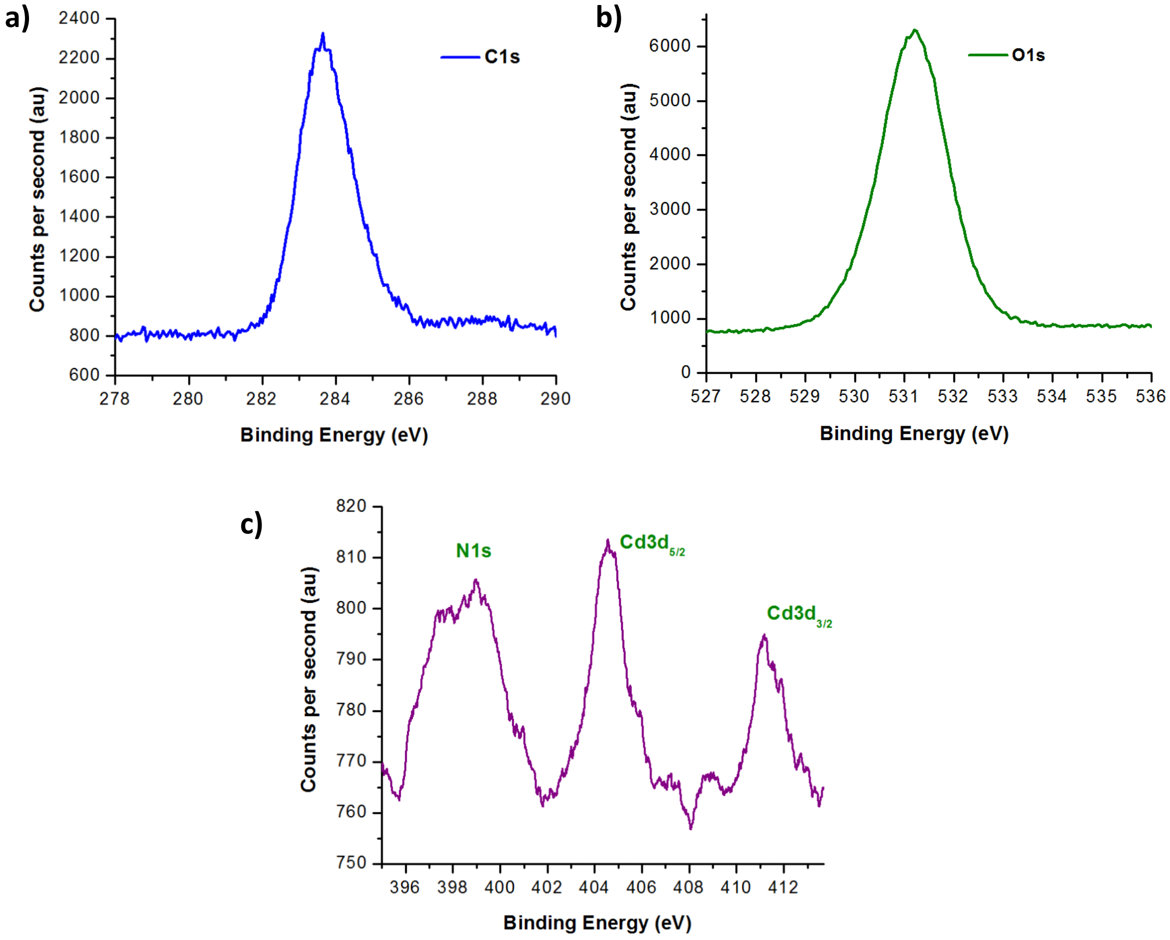

Figure S31. X-ray photoelectron spectrum (XPS) of the exfoliated ethanolic colloidal solution of **Cd-TPA** deposited over silicon wafer. Notice the presence of peaks corresponding to binding energy of a) C1s, b) O1s, c) N1s, Cd($3d_{5/2}$) and Cd($3d_{3/2}$).